THE SEISMOACOUSTIC WAVEFIELD: A NEW PARADIGM IN STUDYING GEOPHYSICAL PHENOMENA

Stephen J. Arrowsmith,[1] Jeffrey B. Johnson,[2] Douglas P. Drob,[3] and Michael A. H. Hedlin[4]

Received 16 March 2010; revised 16 July 2010; accepted 11 August 2010; published 4 December 2010.

[1] The field of seismoacoustics is emerging as an important discipline in its own right, owing to the value of colocated seismic and infrasound arrays that sample elastic energy propagating in both the solid Earth and the atmosphere. The fusion of seismic and infrasonic data provides unique constraints for studying a broad range of topics including the source physics of natural and man-made events, interaction of mechanical waves in Earth's crust and atmosphere, source location and characterization, and inversion of atmospheric and shallow subsurface properties. This review article traces the seismoacoustic wavefield from source to receiver. Beginning at the source, we review the latest insights into the physics of natural and anthropogenic sources that have arisen from the analysis of seismoacoustic data. Next, a comparative review of 3-D models of the atmosphere and solid Earth and the latest algorithms for modeling the propagation of mechanical waves through these media provides the framework for a discussion of the seismoacoustic path. The optimal measurement of seismic and acoustic waves, including a discussion of instrumentation, as well as of array configurations and regional networks, is then outlined. Finally, we focus on broad research applications where the analysis of seismoacoustic data is starting to yield important new results, such as in the field of nuclear explosion monitoring. This review is intended to provide a primer on the field of seismoacoustics for seismologists or acousticians, while also providing a more general review of what constraints seismoacoustics can uniquely provide for understanding geophysical phenomena.

Citation: Arrowsmith, S. J., J. B. Johnson, D. P. Drob, and M. A. H. Hedlin (2010), The seismoacoustic wavefield: A new paradigm in studying geophysical phenomena, *Rev. Geophys.*, *48*, RG4003, doi:10.1029/2010RG000335.

1. INTRODUCTION

[2] Seismologists study seismic waves through geological materials, while the equivalent study of acoustic waves through air is conventionally undertaken by atmospheric physicists. The solid-gas boundary between the lithosphere and atmosphere has thus acted as an intellectual boundary between two disciplines. However, this intellectual boundary is a human construct: both seismic and acoustic/infrasonic waves are mechanical waves that are often generated by the same physical phenomena. The Earth's surface is not opaque to mechanical waves, either those propagating upward from within the Earth's solid interior or those propagating down from the atmosphere. This article is motivated by the need to reconcile these two disciplines for studying physical phenomena that occur on or near the solid Earth–atmosphere boundary.

[3] To illustrate this intellectual boundary, it is worthwhile to consider the practical problem of monitoring nuclear tests. The Comprehensive Nuclear-Test-Ban Treaty (CTBT) bans all nuclear explosions in the atmosphere, in the oceans, and underground. In the current international monitoring regime, the International Monitoring System (IMS) seismic network provides the primary tool for monitoring underground tests, the associated infrasound network is designed for monitoring atmospheric tests, and the hydroacoustic network allows for monitoring of tests in the oceans. Each system was originally conceived to operate largely autonomously.

[4] The difficulty begins when an "event" happens. The event may be an earthquake, for example, a routine mining explosion, or an underground nuclear test. Seismic observations of underground events often do not provide conclusive evidence for discriminating between these different types of events because the geological structure between source and receiver acts as a filter that distorts the waveform. However,

[1]Los Alamos National Laboratory, Los Alamos, New Mexico, USA.
[2]Department of Earth and Environmental Science, New Mexico Institute of Mining and Technology, Socorro, New Mexico, USA.
[3]Space Science Division, U.S. Naval Research Laboratory, Washington, D. C., USA.
[4]Laboratory for Atmospheric Acoustics, Institute of Geophysics and Planetary Physics, Scripps Institution of Oceanography, University of California, San Diego, La Jolla, California, USA.

8755-1209/10/2010RG000335
Paper number 2010RG000335

whereas earthquakes can occur down to depths of up to several hundred kilometers, anthropogenic events are limited to the upper 5 km. At these shallow depths, seismoacoustic wavefields (comprising seismic waves in the solid Earth and acoustic waves in the atmosphere) can be readily generated. For example, infrasonic signals from underground nuclear tests at the Nevada test site were routinely recorded [*Whitaker et al.*, 1992]. Coupled acoustic-to-seismic signals originating from atmospheric events commonly register above noise on seismometers [*de Groot-Hedlin et al.*, 2008; *Kanamori et al.*, 1991]. With two independent measures of the source, the problem of source identification becomes more tractable. For example, as noted above, the very presence of an infrasound signal is indicative of a shallow depth (at least for small- to moderate-sized seismic events), favoring an anthropogenic cause. More generally, the utilization of signals through different media can provide much more rigorous assessment (and removal) of path effects and thus more substantive evidence for political/legal purposes.

[5] The study of seismoacoustics extends far beyond the problem of monitoring nuclear explosions. Seismoacoustics can be utilized to improve our understanding of the source physics of near-surface and surface processes including volcanoes, earthquakes, ocean processes, and many other natural and man-made events. The first part of this article summarizes some seismoacoustic sources, by considering a selection of some of the most important. Next, with a goal of unifying our study of seismic and acoustic wavefields, we compare and contrast 3-D models of the solid Earth and atmosphere, as well as the propagation of mechanical waves through these media. Finally, we outline the seismoacoustic receiver, along with some new findings that have been made on the basis of recent deployments.

2. SEISMOACOUSTIC SOURCES

[6] A common feature of seismoacoustic sources is the excitation of mechanical waves in the solid Earth and atmosphere. Thus, such sources tend to be located at or near the solid Earth–atmosphere boundary. This section summarizes five major seismoacoustic sources.

2.1. Volcanoes

[7] Restless volcanoes radiate seismic energy due to brittle failure of rocks, fluid advection, and opening and resonance of cracks and conduits [*McNutt*, 2005]. When these sources occur at or near the volcanic vent, the atmosphere can be significantly perturbed, and infrasonic waves are generated. Sound waves from varied volcanic activities span a wide range of amplitudes, from tens of mPa to kPa (when reduced to 1 km) [*Johnson et al.*, 2004]; however, much of this energy is peaked in the near-infrasound band (several seconds to ~10 Hz). The prevalence of near-infrasound is due to the accelerations of the atmosphere, which are relatively slow (occurring on time scales of a few tenths to few seconds), and the source dimensions, or vent sizes, which are relatively large (ranging from a few meters to a few hundred meters). For this reason, the corresponding audible sound power spectral density produced during eruption is generally 1–2 orders of magnitude less intense.

[8] Many types of surface eruptive phenomena, ranging from the passive degassing of a lava lake to explosive eruptions from a silicic dome, produce conjoint seismic and infrasonic wave generation [*Marchetti et al.*, 2009]. The seismic waves are propagated into a heterogeneous volcanic medium and are subject to complex Green's functions, while the volcano infrasound radiated to local distances (defined here as on the flanks of the volcano, less than ~10 km) is less affected by atmospheric structure. Compared to the seismic site response, infrasound site responses are also generally minor, as evidenced by volcano infrasound deployments which tend to show self-similar waveforms across a network [*Gresta et al.*, 2004; *Ruiz et al.*, 2006]. For subsonic eruptions, this allows local infrasound records to be scaled back to the vent to infer the acceleration of the atmosphere at the infrasound source. In many studies, the acoustic and seismic sources are considered compact or small with respect to the peak radiated elastic wavelengths. Under these assumptions infrasound waveform inversions can then be used to quantify the acceleration of the atmosphere due to several types of "primary" volcano physical sources including explosive gas release [*Johnson et al.*, 2004; *Oshima and Maekawa*, 2001], the oscillations of large bubbles rising and/or expanding at the surface of a lava lake [*Vergniolle et al.*, 2004], or movements of a solid lava dome [*Yokoo et al.*, 2009].

[9] In a few documented instances, such as at the 200 m diameter dome of Santiaguito, the size of the volcano acoustic source may be larger than the generated sound wavelengths and must be considered as a finite combination of sources [*Johnson and Lees*, 2010]. More commonly, volcanoes, such as Etna or Stromboli, radiate sound simultaneously from a number of vents, which are spatially distributed and considered as independent point sources. In this scenario, both local infrasonic networks [*Cannata et al.*, 2009] and arrays [*Ripepe and Marchetti*, 2002] are effective at distinguishing activity at the various vents. Corresponding seismic arrivals are much harder to use for precise source localization because volcano seismicity, except in the very long period band, is often poorly correlated across a network. In particular, it is difficult to identify correlated phases for emergent or sustained seismic signals. Moreover, the speed of seismic waves in a heterogeneous volcano is often poorly constrained and generally about an order of magnitude faster than sound speeds in the atmosphere. Relative to infrasound locations the seismic spatial source uncertainty is exaggerated for imprecise phase picks.

[10] Secondary sources of volcano infrasound and seismicity have also been widely observed. Spindle-shaped broadband seismic tremor is characteristic of gravity currents, such as pyroclastic flows, rockfalls, or lahars, but is difficult to locate with great accuracy [*Battaglia and Aki*, 2003]. In the infrasonic wavefield, rockfall and pyroclastic flows radiate relatively low intensity infrasonic tremor, but the tremor can often be well tracked with local infrasound arrays or networks [*Ripepe et al.*, 2009; *Yamasato*, 1997]. Other secondary sources of volcano infrasound, such as sound produced

by volcanic lightning or volcanic earthquakes occurring at depth, presumably exist but have not been a focus of previous studies.

[11] The source of most high-amplitude volcano infrasound is confined to volcanic vents, and seismoacoustic observations have been used to infer the depth of sources within a volcanic conduit. Many studies infer that seismic and infrasound radiation can originate from a conjoint fragmentation event, whose depth can be tracked using the relative infrasound and seismic phase arrivals at local stations [*Ripepe et al.*, 2002; *Ruiz et al.*, 2006]. For instance, during the course of an eruption sequence, increasing delay times between seismic and acoustic phases may suggest deepening of the fragmentation source.

[12] The partitioning of elastic energy into the ground and atmosphere is another metric that has been used to understand the nature of coupled seismoacoustic sources. Variations in the ratio of seismic-to-acoustic energy occur rapidly [*Johnson and Aster*, 2005], over the course of seconds to minutes, and have been attributed to variable depth sources and changing acoustic properties of the fluid-filled conduit (lower impedance of the conduit impedes seismic energy radiation) [*Hagerty et al.*, 2000], as well as to variations in eruption style (infrasound radiation may be "muffled" by dense pyroclastic or ash-rich emissions or by a conduit choked with talus) [*Mori et al.*, 1989]. Some events that produce significant seismicity but no corresponding infrasound can intuitively be attributed to earthquake sources that are deeper, or more "muffled," within the interior of a volcano. Generally, recorded eruption infrasound is far more intense than the infrasound predicted by incident seismic waves impinging upon the free surface from an earthquake source occurring at depth.

[13] Linear volcano infrasound sources have typically been modeled as monopole (volumetric) or dipole (momentum imparted to the atmosphere). An example of monopole radiation would be a discrete explosion at the free surface, whereas jetting may be idealized as dipole or even quadrupole radiation [*Woulff and McGetchin*, 1976]. With the exception of some very short lived Strombolian-style eruptions, most eruptions are extended in time (seconds to hours) and likely represent a superposition of explosion and jetting activity. Of the competing sound production mechanisms, monopole radiation, which is isotropic, is far more efficient at producing sound for a given eruption size.

[14] In the case of a monopole source it is useful and straightforward to characterize the acoustic power produced by the volcano, which is proportional to the square of the recorded pressure p at distance r divided by the impedance ρc of the atmosphere:

$$P(t) = \Omega \frac{\overline{p^2(t + r/c)}}{\rho c}. \quad (1)$$

For isotropic radiation into a whole space the surface normal to radiation Ω at radius r is $4\pi r^2$, but for sound confined to the atmosphere above a volcano the solid angle is more limited, e.g., $2\pi r^2$ (half-space) to $3\pi r^2$ (stratovolcano with 30° slope). Dipole radiation is anisotropic with maximum pressure field located along the axis of the dipole. Jet noise has been suggested as a component of the sound field at Mount St. Helens in 2005 [*Matoza et al.*, 2009] and has been used to infer gas jet velocities at Augustine in 2006 [*Caplan-Auerbach et al.*, 2010].

[15] For isotropic or simple volumetric sources recorded locally, infrasound amplitude is conveniently quantified by its reduced pressure, which follows from the assumption that excess pressure falls off as $1/r$. In this case pressure records can be reduced to

$$p_{\mathrm{red}} = p \frac{r}{r_{\mathrm{red}}}, \quad (2)$$

where the reduced distance is often standardized at 1 km. This reduced amplitude is analogous to body wave reduced displacement [*Aki and Koyanagi*, 1981], often used in volcano seismology to compare eruption amplitudes for a suite of eruptions at a single volcano or between many volcanoes.

[16] While the infrasound source is typically characterized by monopole or dipole representations, the corresponding seismic source occurring in a solid or fluid medium is often more complex and may represent a superposition of source types. Thrust response of a volcano edifice, during eruption, may result in a single force directed downward, but moment tensor inversion also indicates that the earthquake associated with eruptions can contain double couple, compensated linear vector dipole, or isotropic contributions [*Chouet*, 2003]. Some of these sources clearly precede the surface manifestation of an eruption by seconds or minutes [*Kobayashi et al.*, 2005] and may indicate fracturing rock, upward advection of gas or magma, or seismoacoustic sources located within the conduit at great depth.

[17] Coupled seismoacoustic observations are important because they provide a comprehensive record of subsurface and eruptive activity. Although some studies have suggested that infrasound is produced by sources immersed in a fluid-filled conduit [*Garcés*, 2000; *Vergniolle et al.*, 1996], recent observations using combined thermal, radar, or visual data streams suggest that high-amplitude infrasound is caused by direct perturbation of the atmosphere [*Johnson*, 2007]. As such, infrasound provides an important record of the varied styles of eruptive activity at diverse volcanoes.

[18] Volcano seismoacoustic records (provided in Figure 1) recorded locally correspond to diverse activity from volcanoes with continuously degassing, low-viscosity lava lakes to activity at dome volcanoes with sticky magmas and episodic ash-rich eruptions. All of these records come from relatively low vigor eruptions at chronically active volcanoes. Although we learn much from these "laboratory" volcanoes, our understanding of volcano infrasound will be stretched when we finally observe large Plinian-style events (i.e., injecting significant ash into the stratosphere) with modern sensors deployed locally and recorded digitally. To date, large eruptions, like Mount St. Helens in 1980 and

Krakatau in 1883, the "loudest natural sound ever produced," have only been documented regionally or globally with analog microbarometers [*Pekeris*, 1939; *Ritsema*, 1980], which are insensitive to the near-infrasound band.

2.2. Earthquakes

[19] Large earthquakes are known to generate seismic and acoustic waves. While the seismic wavefield from earthquakes is comparatively well understood, the corresponding

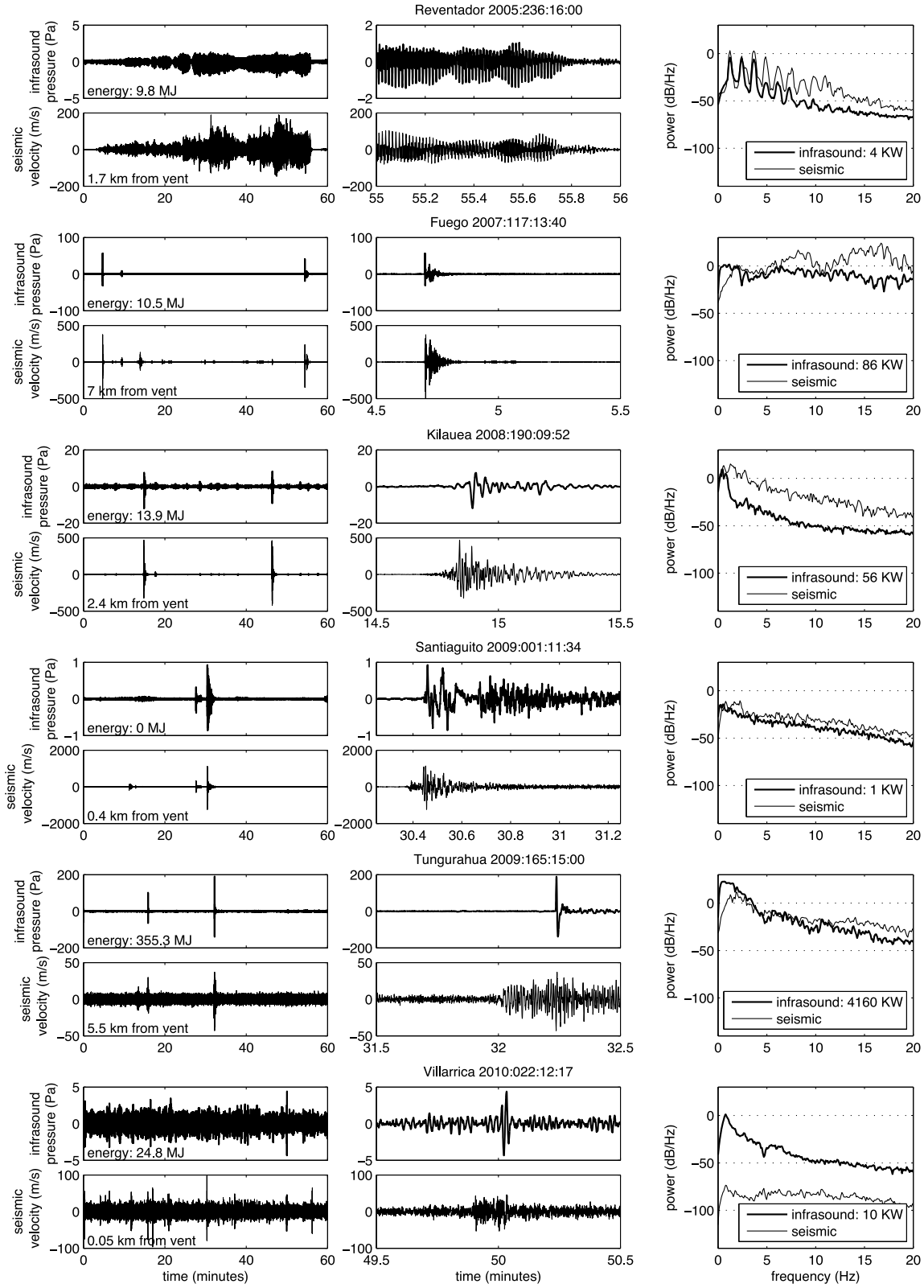

Figure 1

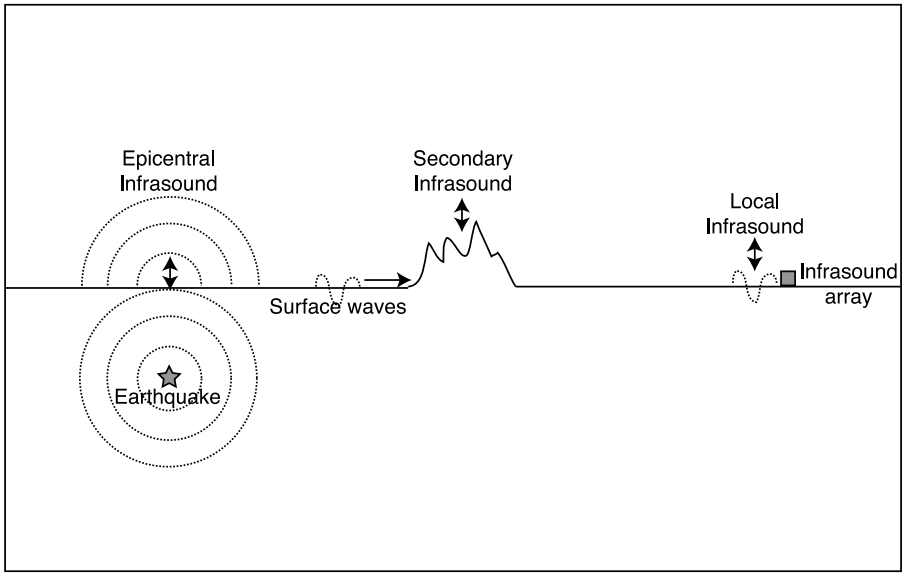

Figure 2. Cartoon illustrating the generation of seismoacoustic signals from earthquakes, which occurs via a variety of interactions between mechanical waves in the crust and atmosphere.

infrasonic wavefield is less well known. However, the fusion of infrasound with seismic data has potential to help improve our understanding of the remote effects of earthquakes on surface motions and to provide new insights into earthquake source physics. The first observations of infrasound from earthquakes were reported by *Benioff and Gutenberg* [1939]. Later, *Bolt* [1964], *Donn and Posmentier* [1964], and *Cook* [1971] reported on the generation of infrasound from vertical ground motion associated with local Rayleigh waves, while *Bolt* [1964], *Mikumo* [1968], and *Young and Greene* [1982] presented observations of infrasound with group velocities consistent with an acoustic source near the epicenter. *Young and Greene* [1982] reported on a third type of signal observed following the great Alaskan earthquake of 1964, which was associated with the passage of seismic waves through the Rocky Mountains. A series of more recent papers [*Arrowsmith et al.*, 2009a; *Le Pichon et al.*, 2002b, 2003, 2005] have confirmed that this third type is caused by vibration of topography and the secondary radiation of acoustic waves into the atmosphere. In this paper, we refer to the first type of infrasound as "local infrasound" (infrasound generated by Rayleigh waves near the receiver), the second type as "epicentral infrasound" (infrasound generated by surface pumping above the epicenter), and the third type as "secondary infrasound" (infrasound generated by the interaction of surface waves with topography or other crustal features such as sedimentary basins) (see Figure 2).

[20] *Mutschlecner and Whitaker* [2005] and *Le Pichon et al.* [2006] have developed preliminary infrasonic earthquake-scaling relationships, which relate the log of the epicentral infrasound amplitude (corrected for stratospheric winds) and the log of epicentral signal duration to earthquake magnitude (Figure 3). The good correspondence between the observations in these two independent studies, which largely focus on different sizes of events, suggests that to first order a linear scaling law governs these relationships for earthquakes from magnitude 4 to magnitude 9. The wind correction, which is based on empirical observations of infrasound from underground nuclear tests [*Mutschlecner et al.*, 1999], appears to be a good approximation for stratospheric phases. Future research is needed to study the relationships between infrasound observables and earthquake depth and mechanism (which are not accounted for by *Mutschlecner and Whitaker* [2005] or *Le Pichon et al.* [2006]), assess the relationship below magnitude 4 (from which there has yet to be a conclusive infrasonic detection), and utilize different infrasonic phases. This work should be performed in parallel with a modeling study in order to better understand the physical basis for these relationships.

[21] Seismoacoustic observations of earthquakes and subsequent research studies have historically been limited because

Figure 1. A sampling of volcano seismoacoustic signals recorded at persistently active, low-vigor eruptions at Reventador (Ecuador), Fuego (Guatemala), Kilauea (Hawaii), Santiaguito (Guatemala), Tungurahua (Ecuador), and Villarrica (Chile). Harmonic tremor at Reventador corresponds to vigorous and rhythmic degassing. Fuego and Tungurahua activities are manifested by Strombolian and Vulcanian blasts. Vigorous degassing from open conduits and lava lakes is shown for Kilauea and Villarrica. Santiaguito signals were recorded during episodic pyroclastic-laden eruptions from the dome. Infrasound pressures have been reduced to 1 km (equation (2)), while seismic velocity amplitudes are given for stations with specified distance to the vent. Hour-long infrasound energy and power spectral density for zoomed in data traces are indicated using equation (3). Seismic power is normalized across the six data sets. All data have been filtered above 0.25 s with a two-pole Butterworth filter to deemphasize microbarom noise.

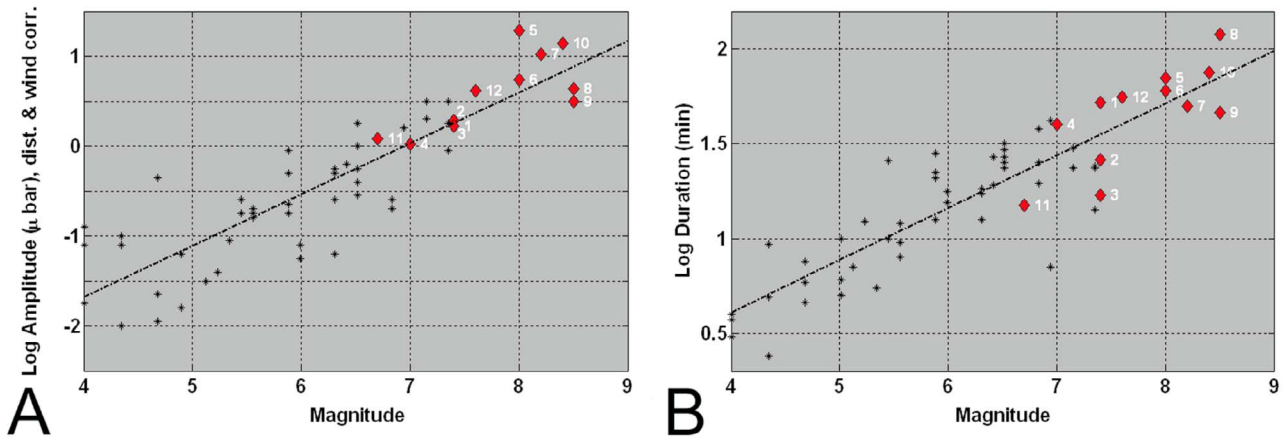

Figure 3. Preliminary scaling laws for earthquake infrasound, comprising observations by *Mutschlecner and Whitaker* [2005] (black points) and additional independent observations of large earthquakes (red points) [from *Le Pichon et al.*, 2006].

of the lack (or sparseness) of infrasound arrays. However, with the recent deployments of the IMS global infrasound network, which complements the associated seismic network, and increased deployments of regional seismoacoustic arrays, these observations are becoming more commonplace. Following the 2004 Sumatra earthquake and tsunami, IMS arrays detected a wealth of infrasonic signals from the earthquake and tsunami [*Garcés et al.*, 2005; *Le Pichon et al.*, 2005].

2.3. Meteors

[22] Large meteoroids can generate seismoacoustic signals as they interact with Earth's atmosphere. Two broad physical processes of airwave generation can occur. First, when meteoroids enter Earth's atmosphere at hypersonic velocity, they generate a shock wave with approximately cylindrical wavefronts [*ReVelle*, 1976]. Second, some meteoroids can suddenly and violently fragment at the point where the structural strength of the meteoroid is less than the air ram pressure [*Bronsthen*, 1983]. When the resultant airwave impinges on the ground, it can couple into the solid Earth, generating seismic waves. The first known seismic observations of a meteoroid were from the Great Siberian Meteor that exploded over Tunguska on 30 June 1908 [*Ben-Menahem*, 1975; *Whipple*, 1930]. An excellent review of seismic observations of meteors is provided by *Edwards et al.* [2008]. In addition to providing constraints on air-ground coupling, seismic observations of meteoroids may provide an invaluable source of data for investigating the seismic properties of the near surface of the Earth [*Langston*, 2004].

[23] Infrasound observations of bolides have been utilized to reconstruct meteoroid trajectories [*Evers and Haak*, 2003; *Le Pichon et al.*, 2002a] and to provide estimates of energy release [*Brown et al.*, 2008]. Infrasound observations of bolides also provide important constraints on the flux of meteoroids that penetrate Earth's atmosphere [*P. Brown et al.*, 2002a]. Because bolides are large explosive events in the atmosphere, they are good natural analogs of nuclear tests in the atmosphere and have been used to validate the IMS infrasound network [*Arrowsmith et al.*, 2008b; *P. Brown et al.*, 2002b].

[24] The combined seismic and infrasonic analysis of bolides has several uses. For example, *Le Pichon et al.* [2008] were able to observe infrasound from the fall of the 15 September 2007 Carancas meteorite and seismic waves caused by the impact with the Earth. *Arrowsmith et al.* [2007] exploited dense seismic observations to accurately constrain the location of the terminal burst of a bolide over Washington State, allowing an assessment of the accuracy with which infrasonic observations at longer-range distances could be modeled. *Hedlin et al.* [2010] used vertical component recordings of acoustic-to-seismic coupled energy made by stations in the USArray transportable array and dense regional seismic networks to study branches of infrasound from a large bolide that burst above Oregon in 2008.

2.4. Explosions

[25] Explosions are efficient sources of seismoacoustic waves. As outlined in detail below, underground nuclear and chemical explosions, nuclear and chemical explosions in the atmosphere, and surface explosions (including mining explosions) can all generate seismic and infrasonic waves.

[26] The explosion of the first Soviet atomic bomb in 1949 spurred research on the use of infrasound for monitoring tests in the atmosphere. Infrasound, because of its ability to propagate long distances, is ideally suited to detecting and locating tests in the atmosphere [*Donn and Ewing*, 1962; *Donn et al.*, 1963; *Wexler and Hass*, 1962]. Atmospheric nuclear tests were also observed seismically [*Toksöz and Ben-Menahem*, 1964]. Following the ratification of the Limited Test Ban Treaty in 1963, which prohibited the testing of nuclear weapons in the atmosphere, space, and the oceans, more emphasis was placed on seismic monitoring of underground tests. However, with the opening for signature of the CTBT in 1996, infrasound technology experienced a renaissance as part of the verification regime. The installation of

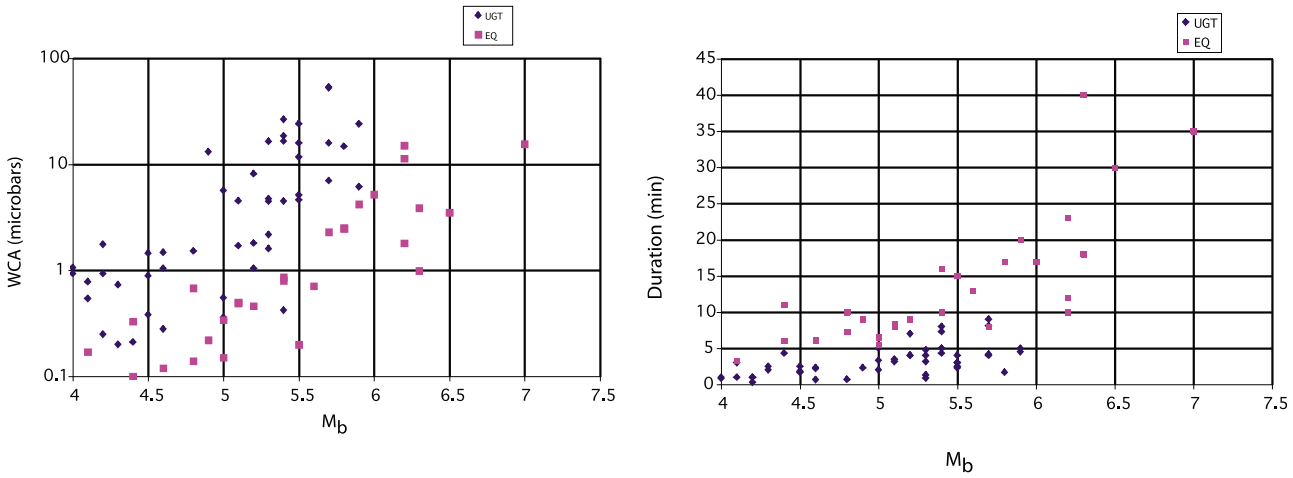

Figure 4. Comparison between infrasonic observations ((left) wind-corrected amplitude and (right) duration) and magnitude for earthquakes (magenta points) and underground nuclear tests (blue points). Courtesy of Rod Whitaker.

the International Monitoring System infrasound network, which comprises 60 infrasound arrays around the globe, is designed primarily to detect nuclear explosions in the atmosphere. A recent study of the capability of the IMS array highlighted that explosions equivalent to ~500 t of TNT in the atmosphere would likely be detected by at least two stations at any time of year [*Le Pichon et al.*, 2009].

[27] The IMS seismic network is designed to detect underground tests. Infrasound is not normally associated with underground nuclear tests, but because of their location near the crust-atmosphere boundary, underground tests can and do generate infrasound. *Whitaker et al.* [1992] report on observations of infrasound from underground nuclear tests conducted at the Nevada Test Site. More recently, *Che et al.* [2009b] presented infrasonic observations from the North Korean nuclear test on 25 May 2009. The first North Korean test on 9 October 2006, which was smaller, was not detected infrasonically. As shown in Figure 4, compared with earthquake observations, infrasound observations of underground nuclear tests are systematically larger in amplitude and shorter in duration [*Whitaker*, 2007].

[28] Mining explosions are commonly detected and reported in regional seismic catalogs below $M = 4.0$. A wide variety of mining explosions can occur [*Stump et al.*, 2002]; among the largest types of mining explosions are the cast blasts, which typically comprise a series of shots detonated in sequence in order to minimize ground motion while maximizing rock fragmentation. The complex source time functions of such explosions can make them appear earthquake-like on seismic waveforms. However, cast blasts generate larger-amplitude infrasound than would be expected for earthquakes of comparable magnitudes [*Arrowsmith et al.*, 2008a; *McKenna et al.*, 2007]. Unfortunately, the studies of infrasound from mining explosions by *McKenna et al.* [2007] and *Arrowsmith et al.* [2008a] were hampered by high noise. Future studies based on observations at low-noise arrays of ground truth events are needed, allowing detailed waveform modeling studies. Observations of infrasound from cast blasts have been used to investigate seasonal variations in detectability, related primarily to seasonal variations in the stratospheric wind jet [*Arrowsmith et al.*, 2008a; *Hagerty et al.*, 2002].

[29] Recent studies have begun to investigate the added value of combining both seismic and infrasonic observations from explosions. *Stump et al.* [2008] deployed a series of seismic and acoustic instruments to record surface explosions in Utah, finding that whereas seismic observations were consistent for each shot, infrasound observations at close range varied considerably. *Gitterman and Hofstetter* [2008] studied seismic and acoustic signatures from a series of explosions in Israel, their findings highlighting clear infrasonic detections at local to regional distances. *Gibbons et al.* [2007] observe seismic and infrasonic signals from more than 100 surface explosions in Finland. A major motivation for combining seismic and infrasonic observations of explosions is to obtain some information on the depth, or altitude, of the explosion. There is often a trade-off between depth and origin time from seismic constraints alone, and infrasound can provide important additional constraints.

2.5. Ocean Noise

[30] Perhaps the most consistent features observed on seismometers and microbarographs around the world are clear spectral peaks between ~0.1 and 0.5 Hz. These peaks are associated with standing waves on the surface of the ocean caused by interfering swells (the source theory is developed by *Longuet-Higgins* [1950] for seismic signals and *Posmentier* [1967] for acoustic signals). On the basis of empirical observations, the seismic waves (termed microseisms) and their corresponding acoustic waves (microbaroms) appear to be generated by the same ocean sources [*Rind*, 1980]. Microseisms and microbaroms are most commonly generated in the North Atlantic and Pacific during the boreal winter and in the southern oceans during the austral winter [*Willis et al.*, 2004], following the seasonal pattern of

oceanic storms. Unlike the other sources discussed in this article, microseisms and microbaroms are continuous signals. Although conventionally regarded as a source of noise, these seismoacoustic signals contain a wealth of information about the nature of these sources, in addition to the atmosphere between source and receiver. *Donn and Rind* [1972] and later *Garcés et al.* [2004] explore the use of microbarom signals to determine continuous measurements of winds and temperatures in the atmosphere. *Barruol et al.* [2006] found that seismic and infrasonic noise amplitudes at stations in French Polynesia correlated with swell amplitudes predicted by NOAA WaveWatch models. The fusion of seismic and acoustic data may be particularly important in inverting for atmospheric winds and temperatures since microseisms may allow for the separation of source and path effects on recorded microbaroms.

[31] A second source of seismoacoustic waves from the ocean is surf. By correlating wave height data from buoys with infrasound measurements, *Garcés et al.* [2003] and *Arrowsmith and Hedlin* [2005] identified surf-related infrasound in Hawaii and Southern California, respectively. Surf infrasound is manifested by clear transient signals at short distances and by continuous hum at regional distances (i.e., >1 stratospheric bounce) but can be distinguished from microbaroms by its frequency content (surf infrasound is dominantly in the 1–5 Hz frequency band). The precise physical mechanism by which breaking waves generate infrasound remains unknown, but a recent study by *Garcés et al.* [2006] confirmed that infrasound may be produced by plunging (or barreling) waves as well as by surf impacting cliffs and exposed reefs. In addition to generating infrasound, surf can be recorded seismically [*Byerly*, 1942; *Hasselmann*, 1963]. The potential for combining seismic and infrasonic constraints to improve our understanding of these signals has not yet been explored.

3. THREE-DIMENSIONAL MODELS

[32] Models of the solid Earth and atmosphere are necessary to correct for path effects on seismoacoustic signals. In addition to differences in spatial resolution, there are two fundamental differences between our models of the solid Earth and atmosphere:

[33] 1. Unlike 3-D models of the Earth, which are primarily constrained by seismic traveltimes, models of the atmosphere used for infrasonic propagation modeling are derived from independent measurements (e.g., satellites and radiosondes).

[34] 2. The atmosphere is temporally variable at the time scale of observation. Consequently, atmospheric models cannot be readily validated empirically in the same manner as seismic models.

[35] These two fundamental differences trade off against each other. Whereas it is a clear advantage to have multiple means of independently measuring atmospheric properties, the difficulty of adequately resolving the temporal variability of the atmosphere has hampered the location and characterization of infrasound events. In some sense, a combined seismoacoustic approach allows us to exploit the unique advantages inherent in our knowledge of the solid Earth and atmosphere. This section summarizes and compares the resolution and fidelity of 3-D models of the Earth and atmosphere.

3.1. Solid Earth

[36] In a broad sense, the 1-D longitudinal and shear wave velocity profiles of the solid Earth are characterized by abrupt discontinuities at the base of the crust, at 410 km and 660 km in the upper mantle, at the base of the lower mantle, and at the base of the outer core. Seismic waves can be refracted or reflected at these boundaries and refracted by gradational variations between these boundaries. In contrast, the atmosphere (described in section 3.2) does not contain comparable sharp discontinuities but is characterized by more gradual fluctuations.

[37] A large body of recent work has looked at lateral heterogeneity in the solid Earth. In a benchmark paper, *Aki et al.* [1977] developed the first 3-D model of mantle heterogeneity using seismic data from the Norwegian Seismic Array in southern Norway, providing the framework for what was to be called "seismic tomography." Since this first study, advances have been made in almost every aspect of the tomography problem, including improved instrumentation, improved earthquake location, more efficient matrix techniques (allowing many more model parameters), improved parameterization schemes, proper treatment of nonlinearity, and the development of corrections for the effect of the crust. The resolution and fidelity of solid Earth models vary around the world, depending on the spatial distribution of seismic sensors. However, global 3-D models now span the entire depth range of the mantle and achieve lateral resolutions corresponding to wavelengths of less than 1000 km [*Romanowicz*, 2003]. Deployments such as the USArray enable enhanced resolutions of <100 km over continental scales [*Burdick et al.*, 2008].

[38] Despite the lack of independent constraints, there is considerable agreement between large-scale features in global tomographic models, with some second-order differences due largely to differences in tomographic approaches [*Becker and Boschi*, 2002]. Furthermore, after applying appropriate damping and/or smoothing constraints, global and regional tomographic inversions typically result in ~80%–90% residual reductions (relative to standard 1-D Earth models). These facts point to the high fidelity of 3-D Earth models today.

[39] Lateral heterogeneity in the solid Earth is typically ±2%–4% in the upper mantle reaching up to ±5% at the base of the mantle. Compared with lateral heterogeneity in the atmosphere, these differences are quite large.

3.2. Atmosphere

[40] Three important variables affect the propagation of infrasound through the atmosphere: temperature, wind speed, and wind direction. The temperature as a function of elevation (Figure 5) is determined primarily by variations in the absorption of solar radiation with height (refer to *Beer* [1974] and *Andrews et al.* [1987] for a more complete review). The atmosphere is conventionally divided into layers based upon

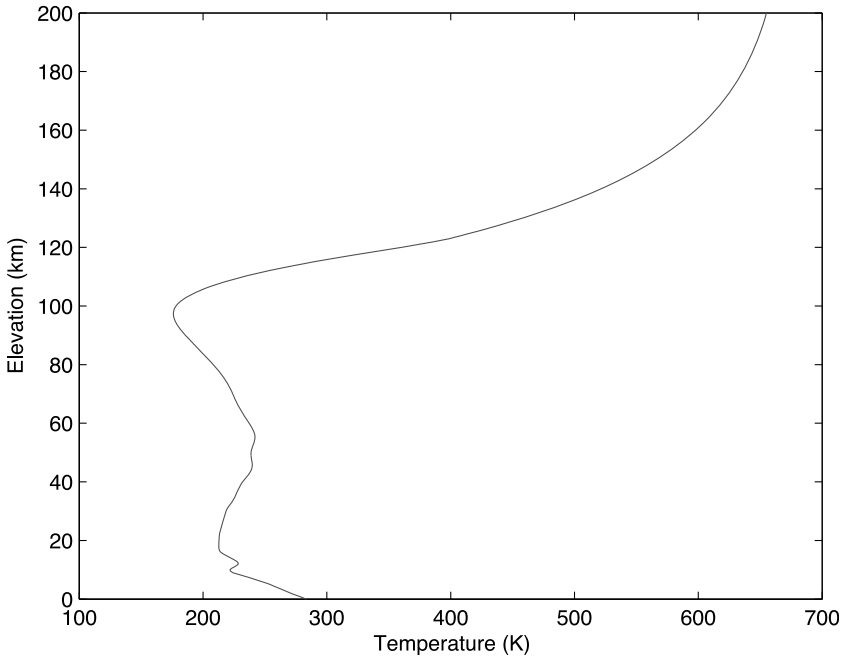

Figure 5. A temperature profile of the atmosphere from the ground to the thermosphere. This temperature profile is extracted for a location at Wells, Nevada, from the Ground-to-Space model for 21 February 2008.

elevations at which the temperature profile changes sign. The lowest layer, the troposphere, usually terminates at heights of ~7–17 km, depending upon latitude and season. The temperature then rises through the stratosphere until the stratopause is reached at ~45–55 km, then declines through the mesosphere until the mesopause at ~80–100 km. Above this height is the thermosphere, which is associated with such a strong increase in temperature that infrasound (unless propagating vertically) does not propagate beyond this region but is refracted back toward the Earth.

[41] The speed of sound, c, for a perfect gas is given by

$$c = (\gamma RT)^{1/2}, \tag{3}$$

where γ is the ratio of specific heats, R is the gas constant, and T is the absolute temperature. Thus, the sound speed is proportional to the square root of the absolute temperature. However, sound propagation in the Earth's atmosphere is also affected by winds as follows:

$$c_{\text{eff}} = c + \mathbf{v} \cdot \mathbf{n}, \tag{4}$$

where $\mathbf{v}$ is the wind vector and $\mathbf{n}$ is the ray normal, their dot product being the wind projection along the propagation path. At first order, the temperature profile can be thought of as dominating the propagation of infrasound, with winds either enhancing or destroying ducts in the troposphere, stratosphere, and thermosphere.

[42] For practical infrasound calculations accurate knowledge of the spatiotemporal variability of the atmosphere is needed to model propagation. When considering near-field acoustic propagation (distances < 50 km), only lower atmospheric specifications up to about 15 km need to be considered. For regional propagation (50–250 km) the stratosphere then becomes important. For long-range propagation (250–2000+ km) the thermosphere is also considered to be important. While the vertical profiles of wind and static sound velocity determine whether ducting will occur locally, horizontal gradients (i.e., changes in the vertical profiles) also become important with increasing range. Another important factor to accurately model infrasound propagation is the accurate specification of the topography [*Arrowsmith et al.*, 2007]. Furthermore, for propagation paths over 750 km the time evolution of the background field may also be important; that is, a four-dimensional model may be required. Time dependence is often overlooked in infrasound propagation calculations. Another factor currently ignored in most infrasound propagation calculations is vertical winds, which may only be a few cm/s, on average, but locally may be 5–10 m/s because of internal gravity wave perturbations and are thus an important effect.

[43] In general, the dynamics of the atmosphere can be described by considering the largest spatiotemporal scales, the seasonal variations, to the smallest, the atmosphere's internal gravity wave spectrum [*Andrews et al.*, 1987; *Holton*, 2004]. In between are the weather systems or Rossby waves described by synoptic-scale meteorology. These waves can easily be resolved with today's operational global medium-range assimilation/forecast models. Just below these scales mesoscale phenomenologies such as maritime temperature inversion layers, land-sea breeze, nocturnal temperature inversions, drainage winds, and squall lines also become important. These can be resolved in today's high-resolution global models or regional mesoscale models. In the middle and upper atmosphere, vertically propagating migrating and

nonmigrating tides, driven by the diurnal solar heating of water vapor and ozone in the lower atmosphere, are a dominant part of the spatiotemporal variability of the atmosphere. These are resolved to some degree in the lower atmosphere by global models, but in the upper mesosphere and lower thermosphere, where their amplitudes are significant, other than published research measurements and empirical models, no daily operational middle and upper atmospheric tidal specifications exist. Last at the smallest scales over all altitudes are internal gravity waves. These waves become increasingly important for infrasound propagation with altitude as gravity wave amplitudes grow exponentially to first order as atmospheric density decreases exponentially. These internal gravity waves include both stationary mountain (Lee) waves generated by wind flow over orography and an ambient nonstationary component generated by a variety of geophysical interactions. The spatiotemporal resolution limits of these waves are generally below the global weather prediction analysis products, but the large-scale gravity waves can be deterministically resolved to some extent in the lower atmosphere by mesoscale models or very high resolution global models. For some applications, these waves can also be represented statistically by subgrid-scale spectral parameterizations.

[44] When one considers various types of atmospheric models that can be used to provide the background fields for modeling infrasound propagation from research to applications, the gamut ranges from direct measurements by radiosondes to first principles "whole atmosphere" models. Often, for planned or known events it may be possible to obtain a nearby one-dimensional radiosonde profile (with altitude coverage up to approximately 35 km) which can then be supplemented with other atmospheric models above 35 km to perform infrasound calculations. Starting with the most primitive of models, this might be the U.S. standard atmosphere, which is global and time independent; a tabular climatology such as the 1986 Committee on Space Research International Reference Atmosphere, which represents the monthly average conditions averaged over longitude but as a function of latitude; or the Horizontal Wind Model (HWM)/Mass Spectrometer Incoherent Scatter (MSIS) empirical climatologies, which include observationally based representations of the seasonal, latitudinal, longitudinal, and local time (tidal) variations of the entire atmosphere at very low resolutions. Below 80 km such climatologies have been superseded by the operational 4× daily global analysis fields from a variety of numerical weather prediction centers.

[45] Today, global analysis fields represent a statistical combination of a large number of direct and indirect satellite, ground-based, and in situ measurements [*Simmons et al.*, 2005; *Wu et al.*, 2002], with additional geophysical constraints provided by the governing equations for global fluid dynamics [*Andrews et al.*, 1987; *Holton*, 2004]. For weather prediction it is important that these observational analysis fields be as accurate as possible as they are used to initialize numerical forecast models. The various numerical weather prediction specifications are widely accepted as providing an accurate representation of the day-to-day and hourly variability of the region at horizontal resolutions better than 1° × 1°. The early mathematical foundation of the various procedures employed by the data assimilation systems to produce these analysis fields is described by *Daley* [1991], with recent developments and techniques given by *Joiner and Da Silva* [1998], *Migliorini et al.* [2008], and *Rabier* [2005]. Discussions of the state of the art in both the available satellite measurements and resulting global data fields are also described by *Manney et al.* [2008], *Schwartz et al.* [2008], *Hoppel et al.* [2008], and the references therein. For example, the European Centre for Medium-Range Weather Forecasts has recently begun to produce specifications based on global satellite temperature soundings up to approximately 80 km altitude (0.01 hPa) at 0.25° × 0.25° resolution. The analysis fields available from the National Weather Service (NOAA) have 0.5° × 0.5° resolution and are publicly available up to 45 km (1 mbar). An example of global surface analysis fields from the Navy Operational Numerical Atmospheric Predication System is shown in Figure 6.

[46] The new NASA Goddard Earth Observing System (GEOS-5) also provides experimental near–real time specifications on 72 layers up to 0.01 hPa, resolving both the troposphere and stratosphere at a resolution of 1/2° × 2/3°. A monumental reanalysis effort by the NASA Global Modeling and Assimilation Office called Modern Era Retrospective-Analysis for Research and Applications was recently completed to provide high-resolution GEOS-5 time series at 6 h intervals from 1978 to the present. Additional research to extend global numerical weather prediction models into the lower thermosphere is described by *Eckermann et al.* [2009], *Akmaev et al.* [2008], and *Richter et al.* [2008].

[47] One important issue regarding these specifications is that above ~35 km the wind fields are derived exclusively from the geophysical fluid dynamic balance of the global pressure fields, which are, in turn, determined from infrared temperature soundings. Diagnostic information does, however, enter indirectly through the observation and inner comparison of the global advection of passive observable tracers such as ozone. Furthermore, these derived wind fields are continuously evaluated against nonoperational research observations when and where they exist. Without directly measured atmospheric wind profiles, the resulting specifications thus may be subject to regional or temporal biases; however, as compared to existing empirical climatologies, the operational specifications are vastly superior. The typical stated geophysical uncertainty of these global numerical weather prediction analysis fields is 1.5 K for temperature and 2 m/s for winds near the surface, increasing to 2.5 K for temperature and greater than 5 m/s near the stratopause. With respect to these uncertainties, although the numerical prediction fields are not climatologies, they do represent regional and temporal averages and as such do not consider mesoscale contrasts and localized wind gusts.

[48] Where reliable operational numerical weather prediction systems are limited to regions below the stratopause, the predominant morphology in the 75–150 km region of the

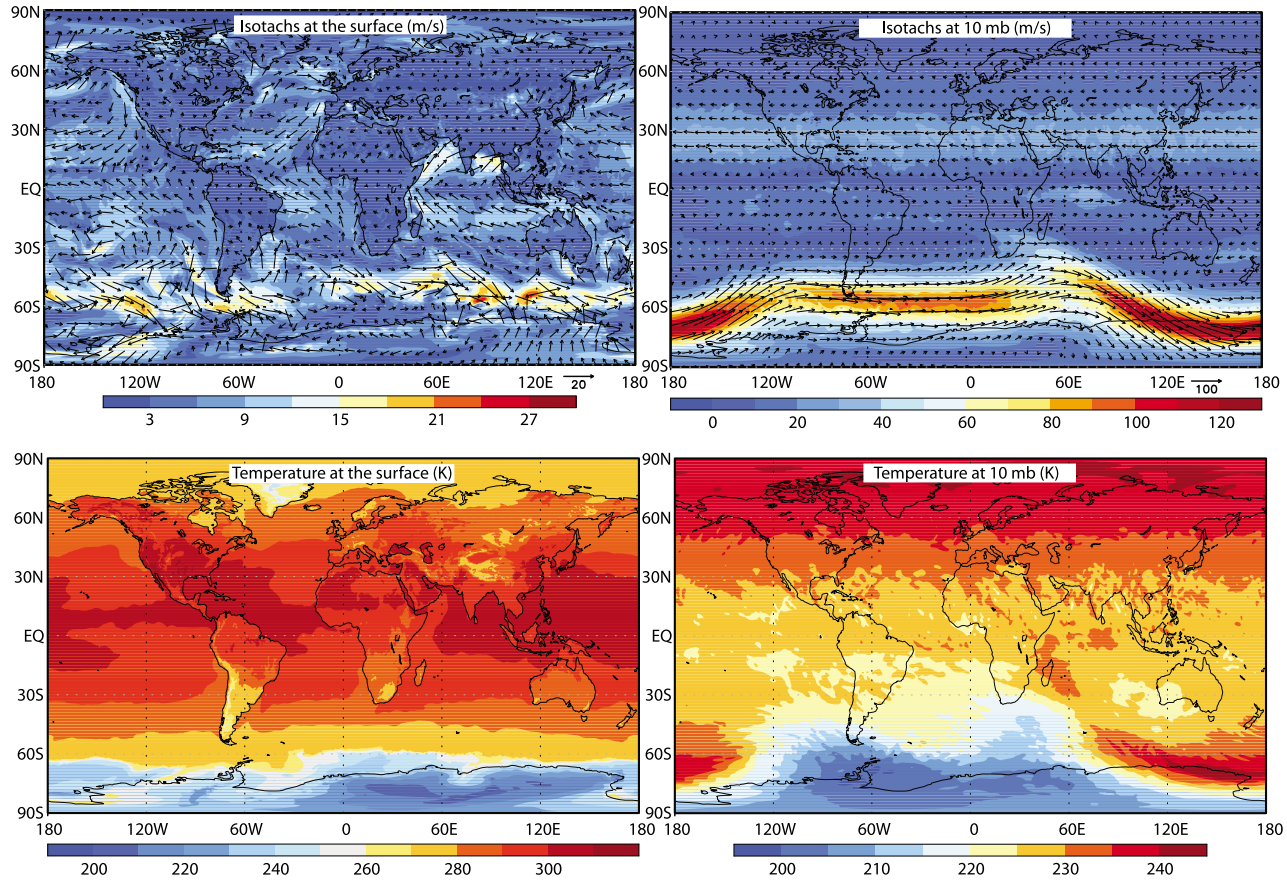

Figure 6. Example analysis fields from the U.S. Navy Operational Numerical Atmospheric Prediction System.

ground-to-space atmosphere is provided by the HWM93 and MSISE-00 empirical models [*Hedin et al.*, 1996; *Picone et al.*, 2002]. These empirical models include statistical parameterizations of the latitudinal, longitudinal, and seasonal variations of the general circulation and temperature structure of the atmosphere, including the diurnal patterns resulting from vertically propagating and in situ driven solar migrating tides. To a large extent the seasonal variations and diurnal patterns dominate the overall morphology of the mesosphere and lower thermosphere. Parameterizations of the effects of solar EUV variability and geomagnetic storms above about 110 km, based on operational space weather indices from NOAA, are also included in the models. These two empirical models are based on 4 decades of satellite, ground-based, and in situ atmospheric measurements, providing a robust statistical synopsis with estimated uncertainties on the order of 20–25 m/s for winds and approximately 10–15 K for temperature in the region between 65 and 120 km. The exact nature of the uncertainties is a function of altitude, local time, latitude, and season. Typically, these uncertainties result from the random geophysical fluctuations occurring on spatiotemporal scales that cannot be resolved by observations assimilated into the empirical model.

[49] The HWM93 model was recently upgraded to HWM07 by *Drob et al.* [2008] via the assimilation of recent upper atmospheric research satellite-based measurements [*Hays et al.*, 1993; *Shepherd et al.*, 1993] and ground-based measurements [*Larsen*, 2002; *Murayama et al.*, 2000; *She*, 2004; *Vincent and Lesicar*, 1991]. The new model provides improved representations of the solar-heating-driven migrating tidal amplitudes and phases, including the seasonal variations thereof. The existing empirical models, however, do not fully include deterministic representations of the day-to-day tidal and planetary wave variability [*Fritts and Isler*, 1994; *Isler and Fritts*, 1995] or, at present, nonmigrating tidal components [*Forbes et al.*, 2003; *Oberheide et al.*, 2006]. When using these empirical models as a proxy for an instantaneous atmospheric profile this geophysical variability accounts for a large portion of the random statistical error.

[50] As mentioned, atmospheric gravity waves in the upper atmosphere provide the second source of geophysical uncertainty for present-day global atmospheric specifications. A large fraction of the gravity wave spectrum in the operational numerical weather prediction models is filtered out during the data assimilation process or simply just not resolved. A recent review of atmospheric gravity waves is provided by *Fritts and Alexander* [2003]. Given the observed and predicted influence of gravity waves on the characteristics of infrasound propagation as described by *Chunchuzov et al.* [2005] and *Kulichkov et al.* [2008], the resolution of these

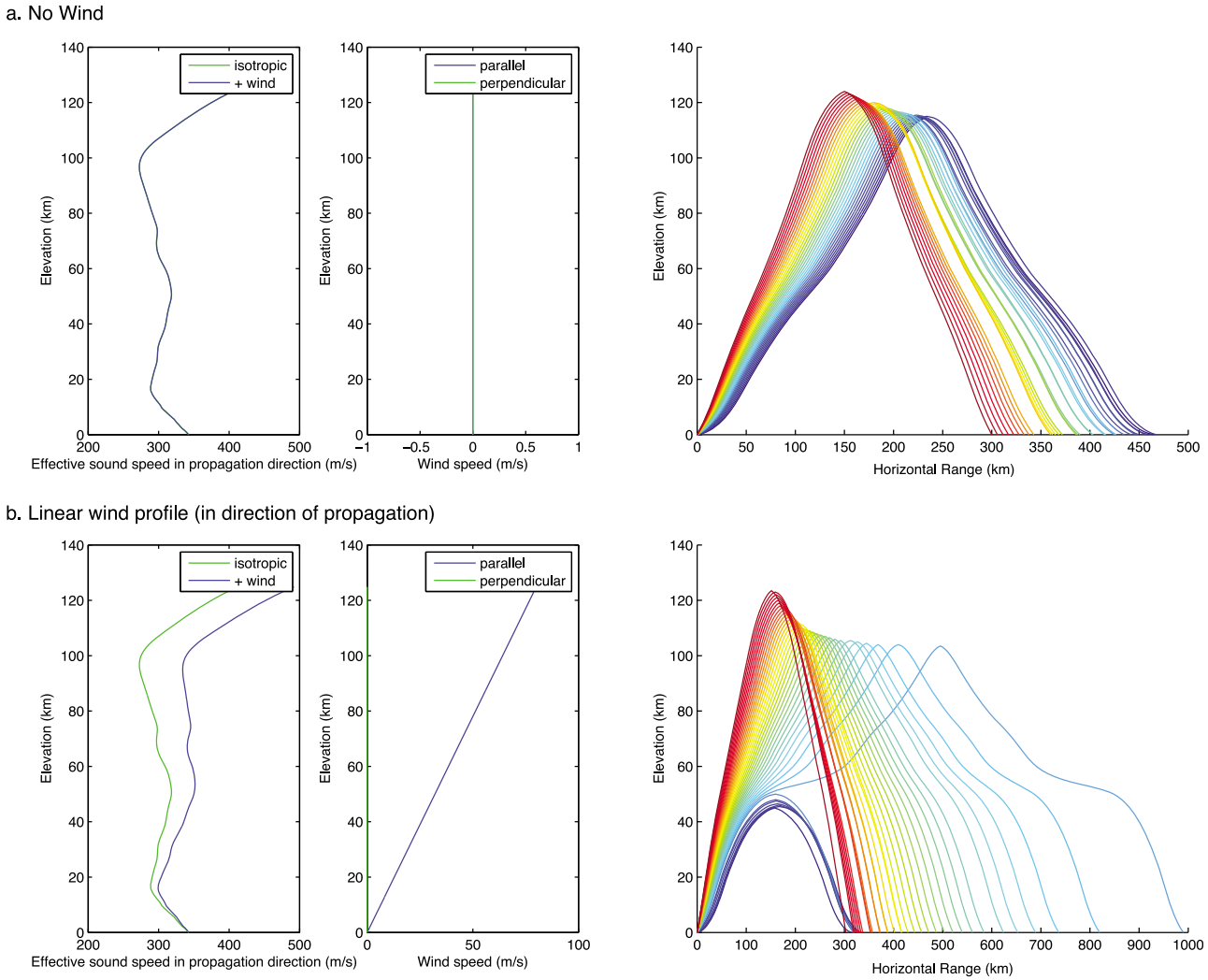

Figure 7. Tau-P simulations showing the effect of wind in the direction of propagation. Refractions occur in the thermosphere in both cases, but the addition of wind enhances the stratospheric duct.

waves through direct measurements or via an adequate semi-empirical spectral parameterization is an important challenge for the infrasound and atmospheric science research community.

4. PROPAGATION OF MECHANICAL WAVES

[51] The physical model for the propagation of seismic and acoustic waves in the far field is the linear wave equation

$$c^2\nabla^2 u - u_{tt} = 0, \tag{5}$$

where u is a physical property associated with the disturbance or signal and c is a constant representing the speed at which the wave travels. The main differences in the propagation of mechanical waves are in differences in the media. For example, for fluids the rigidity (μ) is zero, and therefore, atmospheric acoustic waves are only associated with longitudinal particle motions. Most notably, acoustic waves are affected by winds, which advect acoustic waves. This section will focus initially on the differences in the propagation of seismic and acoustic waves in terms of ray theory, which provides a relatively simple and intuitive summary of the effect of winds on infrasonic propagation, before summarizing some other important differences.

4.1. Solid Earth

[52] As shown by *Lay and Wallace* [1995], the following two equations can be derived from the wave equation under the assumptions inherent in geometric ray theory for a simple 1-D velocity model, with the raypath confined to the x-z plane. These two equations provide the range traversed by the ray X and the corresponding traveltime T in terms of the slowness, $s = 1/c(z)$, and the ray parameter, $p = \sin(\theta)/c(z)$:

$$X = 2p\int_0^z \frac{dz}{\sqrt{s^2 - p^2}} \tag{6}$$

$$T = 2\int_0^z \frac{s^2}{\sqrt{s^2 - p^2}}dz. \tag{7}$$

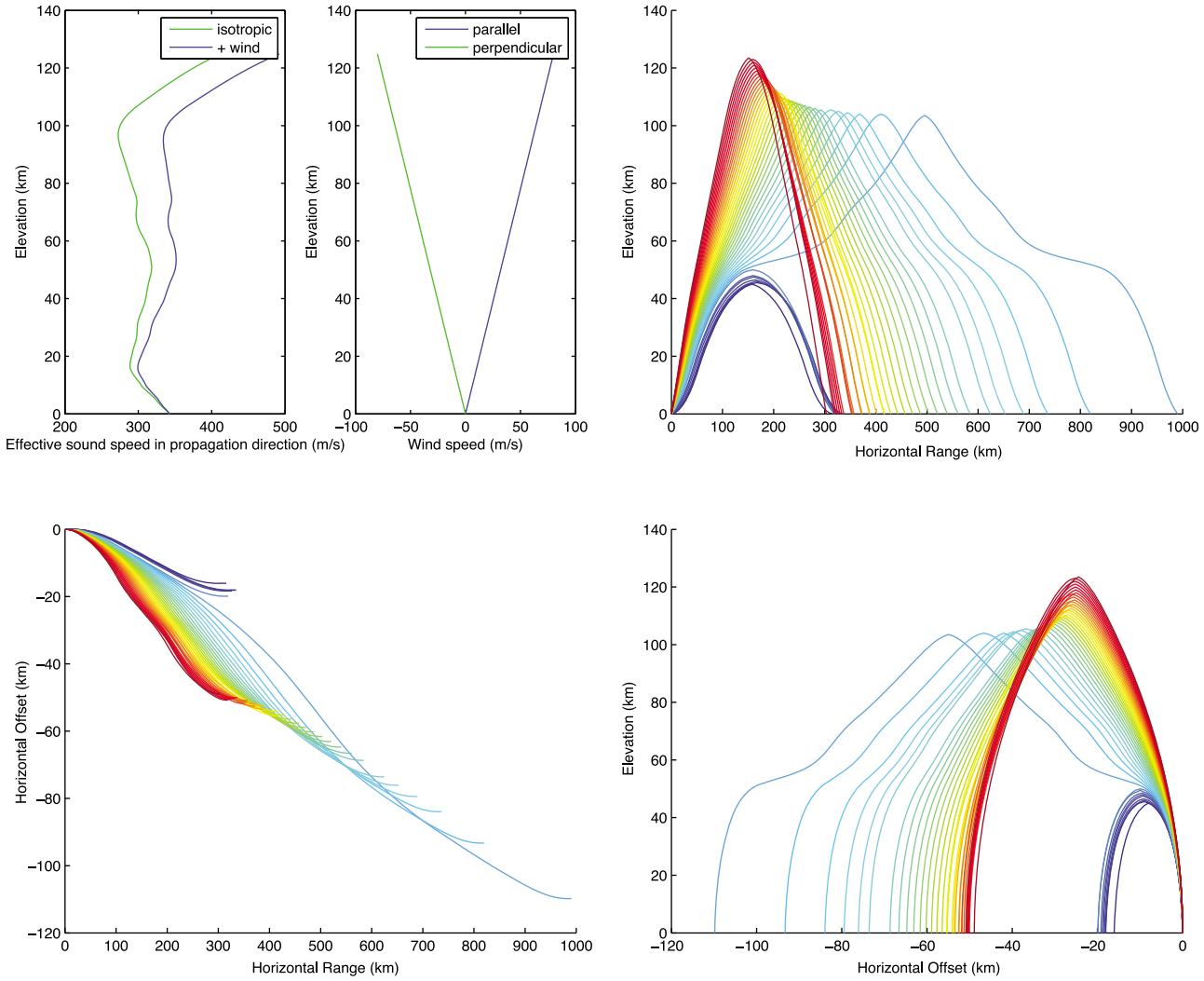

Figure 8. Tau-P simulations showing the effect of wind perpendicular to the direction of propagation.

4.2. Atmosphere

[53] Similar equations can be derived for the propagation of infrasonic waves in the atmosphere, under the same assumptions, with the additional requirement that the wind must be accounted for. Following *Garcés et al.* [1998], in the presence of wind, the propagation of infrasound through a 1-D atmospheric model can be written as

$$X = 2\int_0^z \Psi\left[\frac{p}{1-pu} + s^2 u\right] dz \tag{8}$$

$$Y = \int_0^z \Psi\left[s^2 v\right] dz \tag{9}$$

$$T = 2\int_0^z \Psi s^2 dz, \tag{10}$$

where

$$\Psi = \left[s^2 - \frac{p^2}{(1-pu)^2}\right]^{-\frac{1}{2}} \tag{11}$$

and $u(z)$ and $v(z)$ represent the wind speeds parallel to and perpendicular to the direction of propagation, respectively. It is straightforward to see that in a windless atmosphere, $u = v = 0$, and these three equations reduce to equations (6) and (7) shown above for the solid Earth.

[54] The effect of wind perpendicular to the direction of propagation is to horizontally translate the raypath. Thus, while the propagation of seismic waves in a 1-D (vertically varying) medium remains in the same plane (which we can set to be the x-z plane without loss of generality), out-of-plane translation must be considered in the case of infrasound (resulting in the addition of a new variable, Y).

[55] A suite of example simulations based on the Tau-P method [*Garcés et al.*, 1998] further illustrates the effect of wind as well as the morphology of infrasound propagation. Utilizing an example 1-D temperature profile, Figure 7 illustrates how the effect of adding wind in the direction of propagation enhances the stratospheric duct. To illustrate the effect of wind perpendicular to the plane of propagation, Figure 8 can be contrasted with Figure 7b (which does not involve any transverse offset).

[56] Three-dimensional simulations of infrasound propagation are performed using essentially the same techniques used in seismology: 3-D ray tracing [*Jones et al.*, 1986], normal modes [*Pierce and Kinney*, 1976], parabolic equations [*Gilbert and White*, 1989] (more commonly used in atmospheric acoustics because of comparatively low gradients of lateral deviations in the atmosphere), and finite difference/element methods [*de Groot-Hedlin*, 2008]. An excellent review of the different techniques utilized in modeling infrasound propagation is provided by *Whitaker and Norris* [2008]. State-of-the-art modeling codes incorporate corrections for terrain, turbulence, and gravity waves. The incorporation of these effects has been shown to be particularly important for predicting observations (for example, *Kulichkov* [2004] discusses the importance of turbulence, *Arrowsmith et al.* [2007] highlight the importance of specular reflections off topography, and *Gibson et al.* [2009] highlight the importance of incorporating gravity wave spectral models). Upwind observations cannot typically be modeled using ray theory, in part because available atmospheric models are heavily smoothed [*Negraru et al.*, 2008].

[57] A difficulty in developing and validating infrasonic propagation models relates once again to the temporal variability of the atmosphere. For example, empirical Green's functions can provide a reliable correction for path effects through the solid Earth. However, the temporal variability of the atmosphere makes such an approach impossible for infrasonic waves. Thus, the atmospheric physics community has relied upon a purely physical (not empirical) approach toward accounting for path effects, with simulation codes only validated using specific ground truth events.

4.3. Morphology of Infrasound Propagation

[58] Seismologists are taught to label arrivals on the basis of the propagation path. While the phase identification problem is much trickier for infrasound than it is in seismology, and therefore, the concept of labeling arrivals may make little sense in practice, infrasonic phases are also typically named according to their propagation path. Purely on the basis of variations in atmospheric temperature with height (Figure 5), which are largely dependent on variations in the absorption of solar radiation, infrasound can be refracted back to the Earth in the troposphere, stratosphere, or thermosphere (Figures 7 and 8 illustrate both stratospheric and thermospheric returns). Following the convention of *D. J. Brown et al.* [2002], these signals are denoted as I_w, I_s, and I_t, respectively. Using representative conditions for different times of year, *Drob et al.* [2003] estimate that up to 30% of infrasound energy is ducted in the troposphere, between 0% and 40% is ducted in the stratosphere, and between 40% and 75% is ducted in the thermosphere. Figure 9 shows the spatiotemporal distribution of these ducting fractions for an arbitrary time of 14 March 2010, 0000 UT. Multiple bounces are common for tropospheric and stratospheric returns but are less likely to be detected for thermospheric returns owing to relatively high absorption in the thermosphere [*Sutherland and Bass*, 2004].

5. SEISMOACOUSTIC RECEIVER

[59] We typically use the term "seismoacoustic receiver" to refer to at least one colocated seismometer and microbarometer. Although seismoacoustic signals can be detected on pure seismic networks [*de Groot-Hedlin et al.*, 2008] or pure infrasonic arrays [*Olson et al.*, 2003], the air/ground coupling response can be difficult to account for, and detection thresholds are much higher. *Stump et al.* [2004] outline a practical framework for the deployment of seismoacoustic sites.

[60] Microbarometers are acoustic transducers that typically produce an electrical signal due to the motion of a diaphragm. A reference backing volume provides the means to determine differential pressure, with the low-frequency cutoff determined by a capillary leak introduced into the backing volume. Thus, the microbarometer is not sensitive to meteorological pressure fluctuations. State-of-the-art microbarometers used in infrasound monitoring are configured to have an essentially flat response in the infrasound band and can sense pressure variations of ~1 mPa.

5.1. Noise Reduction

[61] A significant difference between seismic and infrasonic signal processing is that the latter typically requires arrays of sensors in order to separate signals from noise (and for phase identification). Wind and turbulence can generate noise with amplitudes and periods that are comparable to infrasonic signals from regional events. Without exploiting the correlation of signals at separate array elements, it can be difficult to separate signal from noise. Most infrasonic detection algorithms are thus based on signal coherence, rather than incoherent power (e.g., short-term average/long-term average), although spectrogram-based detectors may allow for incoherent detection of explosions [*Taylor et al.*, 2010]. Clearly, the presence of a seismic signal also plays an important role in distinguishing acoustic signals and noise.

[62] A second design feature that is typically deployed is some sort of additional wind-reducing mechanism. Such mechanisms typically take one of two forms, compared by *Hedlin and Raspet* [2003]: (1) a physical shelter placed over the sensor to block wind and (2) a spatial averaging filter that averages pressure fluctuations over some area. As shown in Figure 10, the use of such wind-reducing mechanisms becomes especially critical as the wind speed increases. The latter technique is based on the fact that signals associated with wind are incoherent at offsets of several meters, while remote sources (i.e., infrasound) can be coherent at hundreds of meters. The two most conventional filter types are pipes fitted with inlet ports [*Hedlin et al.*, 2003] and porous hoses [*Stump et al.*, 2004]. Of the two types, porous hoses are not favored for long-term deployments because of concerns about changes in the microporosity with long exposure to UV, although the ease of deployment (and low material cost) makes them a preferred choice for shorter-term deployments. Acoustic impedance contrasts inside pipe filters are known to give

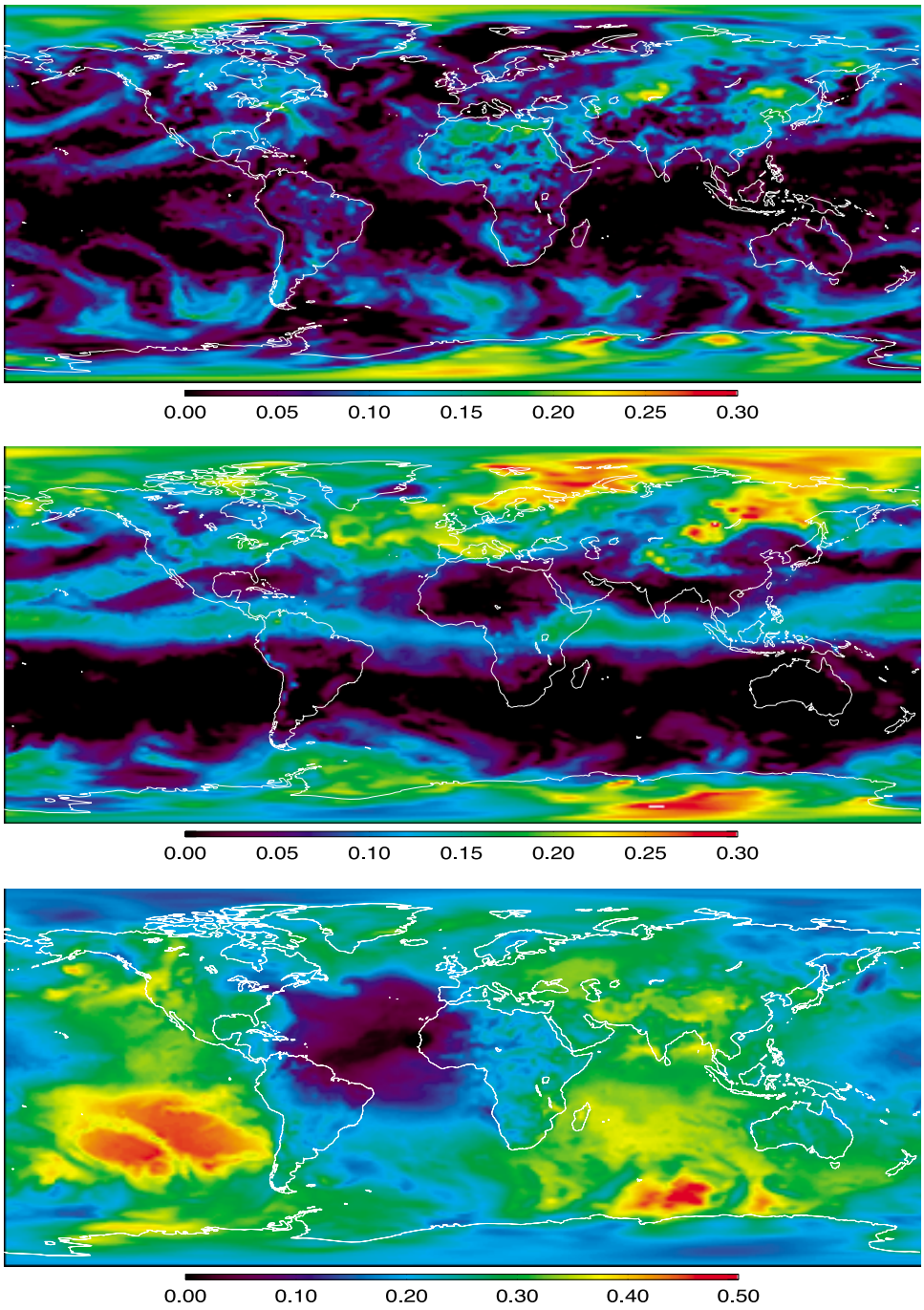

Figure 9. Estimates of the tropospheric, stratospheric, and thermospheric ducting fractions for 14 March 2010, 0000 UT [after *Drob et al.*, 2003].

rise to spectral peaks in the band of interest [*Hedlin et al.*, 2003], although resonance can be removed with appropriate impedance-matching capillaries [*Hedlin and Alcoverro*, 2005]. Other promising methods for reducing atmospheric noise involve integrating atmospheric pressure variations, and thus reducing incoherent noise, along curved or straight lines at light speed using fiber optics [*Zumberge et al.*, 2003] or applying adaptive beam-forming methods to data from very dense arrays of microphones [*Shields*, 2005]. Another promising method for reducing wind noise solution is the pure state filter [*Olson*, 2004]. Perhaps the simplest solution to wind noise reduction is to place the array in dense vegetation, although this is not always practical for every deployment.

5.2. Example Deployments

[63] A series of seismoacoustic deployments have motivated recent interest in the subject. *Stump et al.* [2004] outlined the design and implementation of a seismoacoustic array in Korea and highlighted the utility of such arrays for detecting seismoacoustic signals from anthropogenic causes. In the Korean peninsula, a region not noted for its

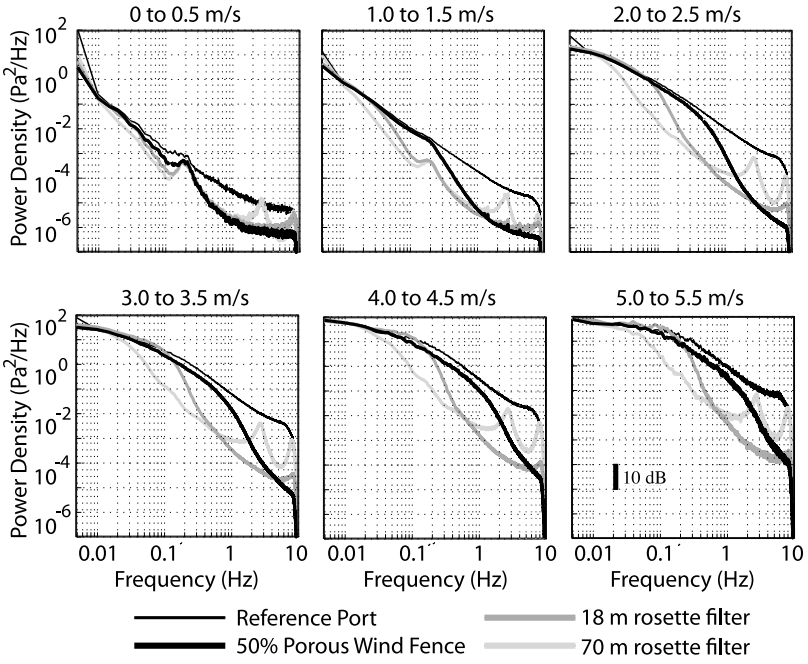

Figure 10. Comparison between the wind noise at various wind speeds recorded on an unprotected microbarometer (reference port) and on microbarometers protected by wind fences or rosette pipe filters (spatial averaging filters). Reprinted with permission from *Hedlin and Raspet* [2003]. Copyright 2003, Acoustical Society of America.

natural seismicity, approximately one fourth of all seismic signals had an associated acoustic signal. *Che et al.* [2002] utilized data from this seismoacoustic array to demonstrate that the combined use of seismic and infrasonic data could be used to discriminate between man-made explosions and earthquakes. Later, using additional seismoacoustic arrays in the Korean peninsula, *Che et al.* [2009a] combined infrasonic constraints with a seismic location scheme and showed that the seismoacoustic locations of ground truth events were more accurate than seismic locations. On the basis of data from these arrays, *Kim et al.* [2004] studied local infrasound signals from the Tokachi-Oki earthquake as a means to quantify the cross coupling from seismic ground motion to infrasound.

[64] Motivated by these deployments in Korea, *Stump et al.* [2007] put out a series of seismoacoustic stations in Utah to study rocket motor explosions from the Utah Test and Training Range. On the basis of these data, considerable variations in infrasonic amplitudes and signal complexity were observed for four identical explosions, which were associated with very similar seismic waveforms [*Stump et al.*, 2008]. These observations, in the local to near-regional distance range, highlighted the importance of capturing the diurnal variability of the atmosphere at these ranges. These findings contrast with earlier studies of stratospheric arrivals from underground nuclear tests [*Mutschlecner et al.*, 1999], which were notable for their temporal consistency.

[65] An exciting prospect for advancing the state of the science is the upcoming colocation of single-channel acoustic sensors with the USArray transportable array, which will effectively provide a dense, semicontinental-scale seismoacoustic network. Clearly, since these sensors will not be installed as arrays, the problem of separating signal from wind noise (discussed in section 5.1) may limit their usage to larger events. The Southern Methodist University group conducted a key pilot experiment in which infrasound sensors were colocated with several stations in the USArray transportable network [*Hayward and Pankow*, 2008; *Rogers et al.*, 2008]. Following the successful conclusion of this experiment, the USArray will be gradually upgraded with infrasound microphones by the University of California, San Diego–Incorporated Research Institutions for Seismology to become entirely seismoacoustic by late 2011/early 2012. The seismoacoustic network will gradually move to the east coast of the continental United States and then to Alaska, allowing the sampling of the seismoacoustic wavefield in different regions at different times of the year.

6. APPLICATIONS

6.1. Nuclear Explosion Monitoring

[66] Recent work has highlighted the potential value of seismoacoustics for nuclear explosion monitoring. There is added value for utilizing both seismic and infrasonic measurements in enhancing the detection, location, and discrimination of events, especially as we move from teleseismic/"telesonic" to local and near-regional distances. While previous methods have been developed primarily for seismic monitoring and then exported to infrasound monitoring, recent work has highlighted the need to develop unique algorithms that exploit the advantages of infrasound while mitigating some of the disadvantages.

6.1.1. Detection

[67] The problem of detecting large, buried, well-coupled underground nuclear tests is trivial. However, for detecting smaller explosions that may not be deeply buried or coupled to the solid Earth, the problem is more difficult using seismic data alone. *Stump et al.* [2004] observed numerous small surface explosions in Korea that were not detected seismically. Clearly, the value of combining seismic and infrasonic data for detection is in detecting events located at or close to the solid Earth–atmosphere boundary.

[68] In seismology, incoherent detectors work quite well. Because of wind noise, which can be as large in amplitude (or sometimes even larger) than the signals of interest, incoherent detectors are unpractical for infrasound data processing. Thus, coherent signal processing, developed for seismic array processing, is typically applied to infrasound data. Unfortunately, coherent "noise" is common on infrasound arrays and arises from a variety of sources including ocean storms, wind farms, and other natural and man-made sources. While such signals may be interesting for their own sake, they are basically noise for the purpose of nuclear explosion monitoring. Recently, *Arrowsmith et al.* [2009b] outlined a new contextual detector (rather than an instantaneous detector that uses only information at a given time instant to determine if a detection has occurred) that adaptively accounts for ambient correlated noise. In the presence of common noise sources such as wind farms, a contextual detector works much better for infrasound processing (Figure 11).

6.1.2. Location

[69] For large events detected at teleseismic distances, there are typically sufficient seismic stations to obtain a reliable location. However, for smaller events that may be detected regionally at only a few seismometers, there is great value in combining seismic with infrasonic observations for localization. In particular, infrasound arrays are more powerful than seismic arrays in providing accurate back-azimuth estimates, owing to the relatively weak lateral heterogeneity of the atmosphere. Furthermore, back-azimuth constraints provide orthogonal information to arrival times for event location [*Modrak et al.*, 2010].

[70] Two problems complicate the infrasound location problem: (1) nonuniqueness of phase identification and (2) limitations in capturing the necessary spatial-temporal characteristics of the atmosphere in atmospheric models. Because of these problems, conventional seismic location techniques are not directly applicable to the atmosphere, at least until the research community has better characterized these limitations. *Modrak et al.* [2010] outline a new approach to infrasound location that incorporates as much robust information as is available into a Bayesian prior term, allowing for the computation of credibility contours (which need not necessarily be ellipsoidal).

6.1.3. Discrimination

[71] In addition to seismic constraints, infrasound observations can provide invaluable additional information for event discrimination. There are two basic approaches to event discrimination that have been explored on the basis of infrasound: (1) source type discrimination and (2) depth discrimination. The first approach attempts to identify infrasonic signatures that are indicative of event type. As shown in Figure 4, *Whitaker* [2009] and *Anderson et al.* [2010] exploit differences in duration and wind-corrected amplitude between earthquakes and underground nuclear tests for event discrimination. Duration is effectively a measure of complexity, earthquakes having more complex source time functions than explosions. Amplitude is indicative of both the depth of an event (explosions are typically shallower than earthquakes) and the source mechanism (e.g., strike-slip earthquakes do not generate surface forcing). The second approach attempts to utilize infrasonic signatures to discriminate shallow earthquakes and explosions from deeper earthquakes and, if possible, to estimate event depth. This latter approach may add independent constraints to seismic estimates of depth, which often trade off with origin time unless a seismic sensor is located above the earthquake origin.

6.2. Volcano Monitoring

[72] Modern volcano monitoring systems utilize an integrated approach that includes both remote sensing and ground-based observations of geodetic anomalies, gas flux anomalies, thermal anomalies, and elastic wave radiation. Traditionally, volcano surveillance has been grounded with in situ seismic networks because they afford a continuous record of earthquakes that occur internally and on the surface of a volcano. Differentiation of various common earthquake types can be used to infer magmatic and hydrothermal fluid movements through conduits and fractures beneath the volcanic edifice [*Chouet*, 1985], shear or tensile failure of the solid rock [*Chouet*, 1979; *Moran*, 1994], very long period volumetric inflations or deflations [*Neuberg et al.*, 1994], and eruption-related phenomena. Local seismic networks distributed around a volcano allow localization of earthquake sources within a volcano and can be used to track magma movement or stress change in the interior of a volcano.

[73] Seismic surveillance is ideally complemented by infrasound monitoring because near-surface activity can also be monitored acoustically in precisely the same band that is targeted for seismic studies [*Matoza et al.*, 2009]. Volcano infrasound has proven beneficial as a hazard monitoring tool because seismic surveillance alone, especially in the short-period band, often cannot distinguish between an explosion earthquake and a subsurface long-period earthquake [*Ruiz et al.*, 2006]. Local infrasound monitoring is particularly effective because the effects of a changing atmosphere, which can influence the radiation of sound at distances as close as ~10 km [*Fee and Garcés*, 2007], are largely minimized. Although infrasound stations may occasionally be obliterated by vigorous volcanic activity [*Moran et al.*, 2008], this detraction can be circumvented by redundant deployment of infrasound at various azimuths and distances as network installations, as is done for seismometers.

[74] Regional and global infrasound monitoring is also capable of providing relatively comprehensive records of eruptive activity. Global observations of very large volcanic events, which have happened perhaps once (at Pinatubo) in the modern digital era (i.e., the last 20 years), were typically

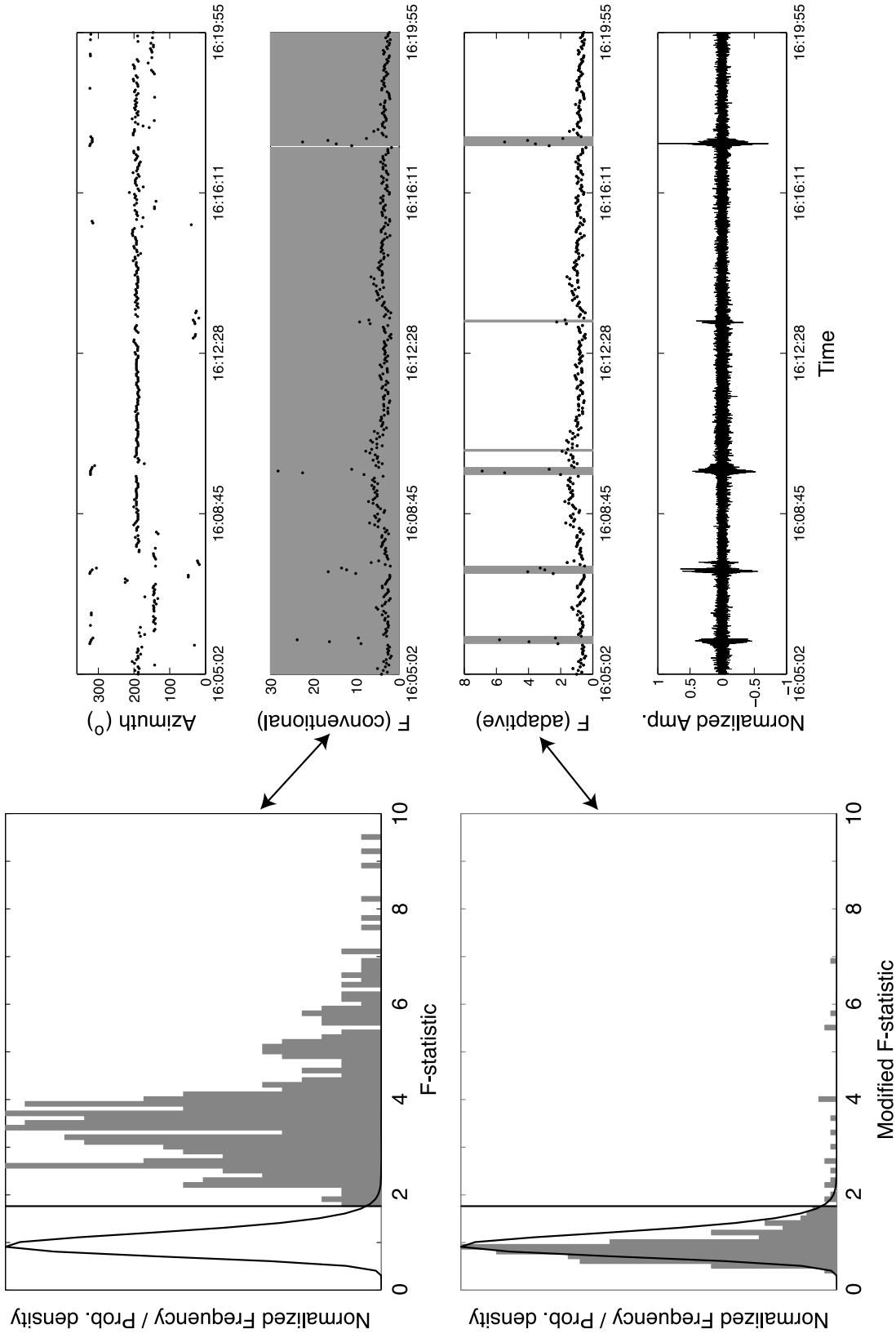

Figure 11. Comparison between the contextual detector (adaptive F-detector) of *Arrowsmith et al.* [2009b] and an instantaneous detector (conventional F-detector) for data corrupted by noise from a wind farm located at an azimuth of 200°.

recorded with microbarometers (e.g., *Strachey* [1888] for the 1883 Krakatau eruption), which had no response in the near-infrasound band but were sometimes used to assess equivalent explosive yields [*Donn and Balachandran*, 1981]. Modern high-fidelity arrays, such as IMS [*Campus*, 2006], research [*Evers and Haak*, 2005; *Wilson et al.*, 2006], and dedicated volcano surveillance arrays, which can affect aviation [*Garcés et al.*, 2007; *Matoza et al.*, 2007], have more recently proven effective at identifying and tracking fluctuations in eruptive activity. The mission of the dedicated regional arrays is to detect ash emissions from volcanoes, which presents a significant hazard for aviation [*Garcés et al.*, 2007]. Regional surveillance is particularly beneficial when resources do not permit local infrasound installations at every potentially active volcano.

7. SUMMARY

[75] In this paper we have attempted to provide a fairly high level overview of the seismoacoustic wavefield from source to receiver and to outline where open research questions can be better addressed by combining seismic and infrasonic measurements. Broadly, the fusion of seismic and infrasonic measurements is useful for studying the source physics of events located at or near the solid Earth–atmosphere boundary; for improving our knowledge of the atmosphere and of Earth structure in the near surface, the so-called seismoacoustic boundary layer [*Langston*, 2010]; and for allowing us to better characterize noise at seismic and infrasound arrays. As demonstrated by the recent research summarized in this article, seismoacoustics has significant potential for improving our capability to monitor for nuclear tests in the solid Earth or atmosphere and for volcano hazard monitoring. With recent deployments, including the modification of the Earthscope transportable array to be fully seismoacoustic, we are primed for advancements in the field of seismoacoustics. However, such advancements will require close collaboration between seismologists and atmospheric physicists, requiring us to bridge the institutional divide between these two disciplines. Our hope is that this article will motivate such bridge building in the future.

[76] **ACKNOWLEDGMENTS.** We gratefully acknowledge Rod Whitaker for providing Figure 4 and for proofreading the manuscript; Kyle Jones for proofreading the manuscript; and the NASA Goddard Space Flight Center, Global Modeling and Assimilation Office, for making the GEOS-5 data available for parts of Figures 6 and 9.

[77] The Editor on this paper was Fabio Florindo. He thanks Maurizio Ripepe and an anonymous reviewer.

REFERENCES

Aki, K., and R. Y. Koyanagi (1981), Deep volcanic tremor and magma ascent mechanism under Kilauea, Hawaii, *J. Geophys. Res.*, *86*, 7095–7109, doi:10.1029/JB086iB08p07095.

Aki, K., A. Christoffersson, and E. S. Husebye (1977), Determination of the three-dimensional seismic structure of the lithosphere, *J. Geophys. Res.*, *82*, 277–296, doi:10.1029/JB082i002p00277.

Akmaev, R. A., T. J. Fuller-Rowell, F. Wu, J. M. Forbes, X. Zhang, A. F. Anghel, M. D. Iredell, S. Moorthi, and H.-M. Juang (2008), Tidal variability in the lower thermosphere: Comparison of Whole Atmosphere Model (WAM) simulations with observations from TIMED, *Geophys. Res. Lett.*, *35*, L03810, doi:10.1029/2007GL032584.

Anderson, D. N., et al. (2010), Seismic event identification, *Wiley Interdiscip. Rev. Comput. Stat.*, *2*, 414–432, doi:10.1002/wics.105.

Andrews, D. G., J. R. Holton, and C. B. Leovy (1987), *Middle Atmosphere Dynamics*, Academic, Orlando, Fla.

Arrowsmith, S. J., and M. A. H. Hedlin (2005), Observations of infrasound from surf in southern California, *Geophys. Res. Lett.*, *32*, L09810, doi:10.1029/2005GL022761.

Arrowsmith, S. J., D. P. Drob, M. A. H. Hedlin, and W. Edwards (2007), A joint seismic and acoustic study of the Washington State bolide: Observations and modeling, *J. Geophys. Res.*, *112*, D09304, doi:10.1029/2006JD008001.

Arrowsmith, S. J., M. A. H. Hedlin, B. Stump, and M. D. Arrowsmith (2008a), Infrasonic signals from large mining explosions, *Bull. Seismol. Soc. Am.*, *98*, doi:10.1785/0120060241.

Arrowsmith, S. J., D. ReVelle, W. Edwards, and P. Brown (2008b), Global detection of infrasonic signals from three large bolides, *Earth Moon Planets*, *102*, 357–363, doi:10.1007/s11038-007-9205-z.

Arrowsmith, S. J., R. Burlacu, R. Whitaker, and G. Randall (2009a), A repeating secondary source of infrasound from the Wells, Nevada, earthquake sequence, *Geophys. Res. Lett.*, *36*, L11817, doi:10.1029/2009GL038363.

Arrowsmith, S. J., R. W. Whitaker, C. Katz, and C. Hayward (2009b), The F-detector revisited: An improved strategy for signal detection at seismic and infrasound arrays, *Bull. Seismol. Soc. Am.*, *99*, 449–453, doi:10.1785/0120080180.

Barruol, G., D. Reymond, F. R. Fontaine, O. Hyvernaud, V. Maurer, and K. Maamaatuaiahutapu (2006), Characterizing swells in the southern Pacific from seismic and infrasonic noise analyses, *Geophys. J. Int.*, *164*, 516–542, doi:10.1111/j.1365-246X.2006.02871.x.

Battaglia, J., and K. Aki (2003), Location of seismic events and eruptive fissures on the Piton de la Fournaise volcano using seismic amplitudes, *J. Geophys. Res.*, *108*(B8), 2364, doi:10.1029/2002JB002193.

Becker, T. W., and L. Boschi (2002), A comparison of tomographic and geodynamic mantle models, *Geochem. Geophys. Geosyst.*, *3*(1), 1003, doi:10.1029/2001GC000168.

Beer, T. (1974), *Atmospheric Waves*, John Wiley, New York.

Benioff, H., and B. Gutenberg (1939), Observations with electromagnetic microbarographs, *Nature*, *144*, 478, doi:10.1038/144478a0.

Ben-Menahem, A. (1975), Source parameters of the Siberian explosion of June 30, 1908, from analysis of seismic signals at four stations, *Phys. Earth Planet. Inter.*, *11*, 1–35, doi:10.1016/0031-9201(75)90072-2.

Bolt, B. A. (1964), Seismic air waves from the great 1946 Alaskan earthquake, *Nature*, *202*, 1095–1096, doi:10.1038/2021095a0.

Bronsthen, V. A. (1983), *Physics of Meteoritic Phenomena*, D. Reidel, Dordrecht, Netherlands.

Brown, D. J., C. Katz, R. Le Bras, M. P. Flanagan, J. Wang, and A. K. Gault (2002), Infrasonic signal detection and source location at the Prototype International Data Center, *Pure Appl. Geophys.*, *159*, 1081–1125, doi:10.1007/s00024-002-8674-2.

Brown, P., R. W. Whitaker, D. ReVelle, and E. Tagliaferri (2002a), Multi-station infrasonic observations of two large bolides: Signal interpretation and implications for monitoring of atmospheric explosions, *Geophys. Res. Lett.*, *29*(13), 1636, doi:10.1029/2001GL013778.

Brown, P., R. E. Spalding, D. ReVelle, E. Tagliaferri, and S. P. Worden (2002b), The flux of small near-Earth objects colliding with the Earth, *Nature*, *420*, 294–296, doi:10.1038/nature01238.

Brown, P., D. ReVelle, E. A. Silber, W. Edwards, S. J. Arrowsmith, L. E. Jackson, G. Tancredi, and D. Eaton (2008), Analysis of a crater-forming meteorite impact in Peru, *J. Geophys. Res.*, *113*, E09007, doi:10.1029/2008JE003105.

Burdick, S., C. Li, V. Martynov, T. Cox, J. Eakins, T. Mulder, L. Astiz, F. L. Vernon, G. L. Pavlis, and R. D. Van der Hilst (2008), Upper mantle heterogeneity beneath North America from travel time tomography with global and USArray transportable array data, *Seismol. Res. Lett.*, *79*, 384–392, doi:10.1785/gssrl.79.3.384.

Byerly, P. (1942), Microseisms at Berkeley and surf on near-by coasts, *Bull. Seismol. Soc. Am.*, *32*, 277–282.

Campus, P. (2006), Monitoring volcanic eruptions with the IMS infrasound network, *InfraMatics*, *16*, 6–12.

Cannata, A., P. Montalto, E. Privitera, G. Russo, and S. Gresta (2009), Tracking eruptive phenomena by infrasound: May 13, 2008 eruption at Mt. Etna, *Geophys. Res. Lett.*, *36*, L05304, doi:10.1029/2008GL036738.

Caplan-Auerbach, J., A. Bellesiles, and J. K. Fernandes (2010), Estimates of eruption velocity and plume height from infrasonic recordings of the 2006 eruption of Augustine Volcano, Alaska, *J. Volcanol. Geotherm. Res.*, *189*(1–2), 12–18, doi:10.1016/j.jvolgeores.2009.10.002.

Che, I.-Y., M.-S. Jun, and J.-S. Jeon (2002), Analysis of local seismo-acoustic events in the Korean Peninsula, *Geophys. Res. Lett.*, *29*(12), 1589, doi:10.1029/2001GL014060.

Che, I.-Y., J. S. Shin, and I. B. Kang (2009a), Seismo-acoustic location method for small-magnitude surface explosions, *Earth Planets Space*, *61*, e1–e4.

Che, I.-Y., T. S. Kim, J.-S. Jeon, and H.-I. Lee (2009b), Infrasound observation of the apparent North Korean nuclear test of 25 May 2009, *Geophys. Res. Lett.*, *36*, L22802, doi:10.1029/2009GL041017.

Chouet, B. (1979), Sources of seismic events in the cooling lava lake of Kilauea Iki, Hawaii, *J. Geophys. Res.*, *84*, 2315–2330, doi:10.1029/JB084iB05p02315.

Chouet, B. (1985), Excitation of a buried magmatic pipe: A seismic source model for volcanic tremor, *J. Geophys. Res.*, *90*(B2), 1881–1893, doi:10.1029/JB090iB02p01881.

Chouet, B. (2003), Volcano seismology, *Pure Appl. Geophys.*, *160*(3), 739–788, doi:10.1007/PL00012556.

Chunchuzov, I., S. Kulichkov, A. Otrezov, and V. Perepelkin (2005), Acoustic pulse propagation through a fluctuating stably stratified atmospheric boundary layer, *J. Acoust. Soc. Am.*, *117*, 1868–1879, doi:10.1121/1.1862573.

Cook, R. K. (1971), Infrasound radiated during the Montana earthquake of 1959 August 18, *Geophys. J. R. Astron. Soc.*, *26*, 191–198, doi:10.1111/j.1365-246X.1971.tb03393.x.

Daley, R. (1991), *Atmospheric Data Analysis*, Cambridge Univ. Press, Cambridge, U. K.

de Groot-Hedlin, C. D. (2008), Finite-difference time-domain synthesis of infrasound propagation through an absorbing atmosphere, *J. Acoust. Soc. Am.*, *124*, 1430–1441, doi:10.1121/1.2959736.

de Groot-Hedlin, C. D., M. A. H. Hedlin, K. T. Walker, D. P. Drob, and M. A. Zumberge (2008), Evaluation of infrasound signals from the shuttle Atlantis using a large-seismic network, *J. Acoust. Soc. Am.*, *124*, 1442–1451, doi:10.1121/1.2956475.

Donn, W. L., and N. K. Balachandran (1981), Mount St. Helens eruption of 18 May, 1980: Air waves and explosive yield, *Science*, *213*, 539–541, doi:10.1126/science.213.4507.539.

Donn, W. L., and M. Ewing (1962), Atmospheric waves from nuclear explosions, *J. Geophys. Res.*, *67*, 1855–1866, doi:10.1029/JZ067i005p01855.

Donn, W. L., and E. S. Posmentier (1964), Ground-coupled air waves from the great Alaskan earthquake, *J. Geophys. Res.*, *69*, 5357–5361, doi:10.1029/JZ069i024p05357.

Donn, W. L., and D. Rind (1972), Microbaroms and the temperature and wind of the upper atmosphere, *J. Atmos. Sci.*, *29*, 156–172, doi:10.1175/1520-0469(1972)029<0156:MATTAW>2.0.CO;2.

Donn, W. L., D. M. Shaw, and A. C. Hubbard (1963), The microbarographic detection of nuclear explosions, *IEEE Trans. Nucl. Sci.*, *10*, 285–296, doi:10.1109/TNS.1963.4323271.

Drob, D. P., J. M. Picone, and M. Garcés (2003), Global morphology of infrasound propagation, *J. Geophys. Res.*, *108*(D21), 4680, doi:10.1029/2002JD003307.

Drob, D. P., et al. (2008), An empirical model of the Earth's horizontal wind fields: HWM07, *J. Geophys. Res.*, *113*, A12304, doi:10.1029/2008JA013668.

Eckermann, S. D., K. W. Hoppel, L. Coy, J. P. McCormack, D. E. Siskind, K. Nielsen, M. Kochenash, M. H. Stevens, and C. R. Englert (2009), High-altitude data assimilation system experiments for the Northern Hemisphere summer mesosphere season of 2007, *J. Atmos. Sol. Terr. Phys.*, *71*, 531–551, doi:10.1016/j.jastp.2008.09.036.

Edwards, W. N., D. W. Eaton, and P. G. Brown (2008), Seismic observations of meteors: Coupling theory and observations, *Rev. Geophys.*, *46*, RG4007, doi:10.1029/2007RG000253.

Evers, L. G., and H. W. Haak (2003), Tracing a meteoric trajectory with infrasound, *Geophys. Res. Lett.*, *30*(24), 2246, doi:10.1029/2003GL017947.

Evers, L. G., and H. W. Haak (2005), The detectability of infrasound in the Netherlands from the Italian volcano Mt. Etna, *J. Atmos. Sol. Terr. Phys.*, *67*(3), 259–268, doi:10.1016/j.jastp.2004.09.002.

Fee, D., and M. Garcés (2007), Infrasonic tremor in the diffraction zone, *Geophys. Res. Lett.*, *34*, L16826, doi:10.1029/2007GL030616.

Forbes, J. M., X. Zhang, E. R. Talaat, and W. Ward (2003), Nonmigrating diurnal tides in the thermosphere, *J. Geophys. Res.*, *108*(A1), 1033, doi:10.1029/2002JA009262.

Fritts, D. C., and M. J. Alexander (2003), Gravity wave dynamics and effects in the middle atmosphere, *Rev. Geophys.*, *41*(1), 1003, doi:10.1029/2001RG000106.

Fritts, D. C., and J. R. Isler (1994), Mean motions and tidal and two-day structure and variability in the mesosphere and lower thermosphere over Hawaii, *J. Atmos. Sci.*, *51*, 2145–2164, doi:10.1175/1520-0469(1994)051<2145:MMATAT>2.0.CO;2.

Garcés, M. (2000), Theory of acoustic propagation in a multiphase stratified liquid flowing within an elastic-walled conduit of varying cross-sectional area, *J. Volcanol. Geotherm. Res.*, *101*(1–2), 1–17, doi:10.1016/S0377-0273(00)00155-4.

Garcés, M., R. A. Hansen, and K. G. Lindquist (1998), Traveltimes for infrasonic waves propagating in a stratified atmosphere, *Geophys. J. Int.*, *135*, 255–263, doi:10.1046/j.1365-246X.1998.00618.x.

Garcés, M., C. Hetzer, M. Merrifield, M. Willis, and J. Aucan (2003), Observations of surf infrasound in Hawai'i, *Geophys. Res. Lett.*, *30*(24), 2264, doi:10.1029/2003GL018614.

Garcés, M., M. Willis, C. Hetzer, A. Le Pichon, and D. P. Drob (2004), On using ocean swells for continuous infrasonic measurements of winds and temperature in the lower, middle, and upper atmosphere, *Geophys. Res. Lett.*, *31*, L19304, doi:10.1029/2004GL020696.

Garcés, M., P. Caron, C. Hetzer, A. Le Pichon, H. Bass, D. P. Drob, and J. Bhattacharyya (2005), Deep infrasound radiated by the Sumatra earthquake and tsunami, *Eos Trans. AGU*, *86*, 317, doi:10.1029/2005EO350002.

Garcés, M., J. Aucan, D. Fee, P. Caron, M. Merrifield, R. Gibson, J. Bhattacharyya, and S. Shah (2006), Infrasound from large surf, *Geophys. Res. Lett.*, *33*, L05611, doi:10.1029/2005GL025085.

Garcés, M., D. Fee, D. McCormack, R. Servranckx, H. Bass, C. Hetzer, M. A. H. Hedlin, R. Matoza, and H. Yepes (2007), Prototype ASHE volcano monitoring system captures the acoustic fingerprint of stratospheric ash injection, *InfraMatics*, *17*, 1–6.

Gibbons, S. J., F. Ringdal, and T. Kvaerna (2007), Joint seismic-infrasonic processing of recordings from a repeating source of

atmospheric explosions, *J. Acoust. Soc. Am.*, *122*, doi:10.1121/1.2784533.

Gibson, R., D. P. Drob, and D. Broutman (2009), Advancement of techniques for modeling the effects of fine-scale atmospheric inhomogeneities on infrasound propagation, in *Proceedings of the 2009 Monitoring Research Review: Ground-Based Nuclear Explosion Monitoring Technologies*, pp. 714–723, Natl. Nucl. Secur. Admin., Washington, D. C.

Gilbert, K. E., and M. J. White (1989), Application of the parabolic equation to sound propagation in a refracting atmosphere, *J. Acoust. Soc. Am.*, *85*(2), 630–637, doi:10.1121/1.397587.

Gitterman, Y., and R. Hofstetter (2008), Infrasound calibration experiment in Israel: Preparation and test shots, in *Proceedings of the 2008 Monitoring Research Review: Ground-Based Nuclear Explosion Monitoring Technologies*, pp. 882–893, Natl. Nucl. Secur. Admin., Washington, D. C.

Gresta, S., M. Ripepe, E. Marchetti, S. D'Amico, M. Coltelli, A. J. L. Harris, and E. Privitera (2004), Seismoacoustic measurements during the July August 2001 eruption of Mt. Etna volcano, Italy, *J. Volcanol. Geotherm. Res.*, *137*, 219–230, doi:10.1016/j.jvolgeores.2004.05.017.

Hagerty, M. T., S. Y. Schwartz, M. Garcés, and M. Protti (2000), Analysis of seismic and acoustic observations at Arenal volcano, Italy, *J. Volcanol. Geotherm. Res.*, *101*, 27–65, doi:10.1016/S0377-0273(00)00162-1.

Hagerty, M. T., W.-Y. Kim, and P. Martysevich (2002), Infrasound detection of large mining blasts in Kazakhstan, *Pure Appl. Geophys.*, *159*, 1063–1079, doi:10.1007/s00024-002-8673-3.

Hasselmann, K. (1963), A statistical analysis of the generation of microseisms, *Rev. Geophys.*, *1*, 177–210, doi:10.1029/RG001i002p00177.

Hays, P. B., V. J. Abreu, M. E. Dobbs, D. A. Gell, H. J. Grassl, and W. R. Skinner (1993), The high-resolution Doppler imager on the Upper-Atmosphere Research Satellite, *J. Geophys. Res.*, *98*, 10,713–10,723, doi:10.1029/93JD00409.

Hayward, C., and K. L. Pankow (2008), Observations of infrasound-to-seismic coupling at Earthscope stations using co located infrasound microphones, *Eos Trans. AGU*, *89*(53), Fall Meet. Suppl., Abstract S33B-1945.

Hedin, A. E., et al. (1996), Empirical wind model for the upper, middle and lower atmosphere, *J. Atmos. Terr. Phys.*, *58*, 1421–1447, doi:10.1016/0021-9169(95)00122-0.

Hedlin, M. A. H., and B. Alcoverro (2005), The use of impedance matching capillaries for reducing resonance in rosette spatial filters, *J. Acoust. Soc. Am.*, *117*, 1880–1888, doi:10.1121/1.1760778.

Hedlin, M. A. H., and R. Raspet (2003), Infrasonic wind-noise reduction by barriers and spatial filters, *J. Acoust. Soc. Am.*, *114*, doi:10.1121/1.1598198.

Hedlin, M. A. H., H. B. Alcoverro, and G. D'Spain (2003), Evaluation of rosette infrasonic noise-reducing spatial filters, *J. Acoust. Soc. Am.*, *114*, doi:10.1121/1.1603763.

Hedlin, M. A. H., D. P. Drob, K. T. Walker, and C. D. de Groot-Hedlin (2010), A study of acoustic propagation from a large bolide using a dense seismic network, *J. Geophys. Res.*, *115*, B11312, doi:10.1029/2010JB007669.

Holton, J. R. (2004), *An Introduction to Dynamic Meteorology*, Elsevier Acad., Burlington, Mass.

Hoppel, K. W., N. L. Baker, L. Coy, S. D. Eckermann, J. P. McCormack, G. Nedoluha, and D. E. Siskind (2008), Assimilation of stratospheric and mesospheric temperatures from MLS and SABER into a global NWP model, *Atmos. Chem. Phys.*, *8*, 6103–6116, doi:10.5194/acp-8-6103-2008.

Isler, J. R., and D. C. Fritts (1995), Mean winds and tidal and planetary wave motions over Hawaii during airborne lidar and observations of Hawaiian airglow Aloha-93, *Geophys. Res. Lett.*, *22*, 2821–2824, doi:10.1029/95GL02186.

Johnson, J. B. (2007), On the relation between infrasound, seismicity, and small pyroclastic explosions at Karymsky Volcano, *J. Geophys. Res.*, *112*, B08203, doi:10.1029/2006JB004654.

Johnson, J. B., and R. C. Aster (2005), Relative partitioning of acoustic and seismic energy during Strombolian eruptions, *J. Volcanol. Geotherm. Res.*, *148*, 334–354, doi:10.1016/j.jvolgeores.2005.05.002.

Johnson, J. B., and J. M. Lees (2010), Sound produced by the rapidly inflating Santiaguito lava dome, Guatemala, *Geophys. Res. Lett.*, doi:10.1029/2010GL045217, in press.

Johnson, J. B., R. C. Aster, and P. R. Kyle (2004), Volcanic eruptions observed with infrasound, *Geophys. Res. Lett.*, *31*, L14604, doi:10.1029/2004GL020020.

Joiner, J., and A. M. Da Silva (1998), Efficient methods to assimilate remotely sensed data based on information content, *Q. J. R. Meteorol. Soc.*, *124*, 1669–1694, doi:10.1002/qj.49712454915.

Jones, M. J., J. Riley, and T. Georges (1986), A versatile three-dimensional Hamiltonian ray-tracing program for acoustic waves in the atmosphere above irregular terrain, report, Wave Propag. Lab., Boulder, Colo.

Kanamori, H., D. Mori, D. L. Anderson, and T. H. Heaton (1991), Seismic excitation by the space shuttle Columbia, *Nature*, *349*, 781–782, doi:10.1038/349781a0.

Kim, T. S., C. Hayward, and B. Stump (2004), Local infrasound signals from the Tokachi-Oki earthquake, *Geophys. Res. Lett.*, *31*, L20605, doi:10.1029/2004GL021178.

Kobayashi, T., Y. Ida, and T. Ohminato (2005), Small inflation sources producing seismic and infrasonic pulses during the 2000 eruptions of Miyake-jima, Japan, *Earth Planet. Sci. Lett.*, *240*(2), 291–301, doi:10.1016/j.epsl.2005.09.015.

Kulichkov, S. N. (2004), Long-range propagation and scattering of low-frequency sound pulses in the middle atmosphere, *Meteorol. Atmos. Phys.*, *85*, 47–60, doi:10.1007/s00703-003-0033-z.

Kulichkov, S. N., I. Chunchuzov, G. A. Bush, and V. Perepelkin (2008), Physical modeling of long-range infrasonic propagation in the atmosphere, *Izv. Russ. Acad. Sci. Atmos. Oceanic Phys.*, Engl. Transl., *44*, 175–186, doi:10.1134/S0001433808020059.

Langston, C. A. (2004), Seismic ground motions from a bolide shock wave, *J. Geophys. Res.*, *109*, B12309, doi:10.1029/2004JB003167.

Langston, C. A. (2010), The seismo-acoustic boundary layer, paper presented at Annual Meeting, Seismol. Soc. of Am., Portland, Oreg., 21–23 April.

Larsen, M. F. (2002), Winds and shears in the mesosphere and lower thermosphere: Results from four decades of chemical release wind measurements, *J. Geophys. Res.*, *107*(A8), 1215, doi:10.1029/2001JA000218.

Lay, T., and T. Wallace (1995), *Modern Global Seismology*, Academic, San Diego, Calif.

Le Pichon, A., J. M. Guerin, and E. Blanc (2002a), Trail in the atmosphere of the 29 December 2000 meteor as recorded in Tahiti: Characteristics and trajectory reconstruction, *J. Geophys. Res.*, *107*(D23), 4709, doi:10.1029/2001JD001283.

Le Pichon, A., J. Guilbert, A. Vega, M. Garcés, and N. Brachet (2002b), Ground-coupled air waves and diffracted infrasound from the Arequipa earthquake of June 23, 2001, *Geophys. Res. Lett.*, *29*(18), 1886, doi:10.1029/2002GL015052.

Le Pichon, A., J. Guilbert, M. Vallee, J. X. Dessa, and M. Ulziibat (2003), Infrasonic imaging of the Kunlun Mountains for the great 2001 China earthquake, *Geophys. Res. Lett.*, *30*(15), 1814, doi:10.1029/2003GL017581.

Le Pichon, A., P. Herry, P. Mialle, J. Vergoz, N. Brachet, M. Garcés, D. P. Drob, and L. Ceranna (2005), Infrasound associated with 2004–2005 large Sumatra earthquakes and tsunami, *Geophys. Res. Lett.*, *32*, L19802, doi:10.1029/2005GL023893.

Le Pichon, A., P. Mialle, J. Guilbert, and J. Vergoz (2006), Multistation infrasonic observations of the Chilean earthquake of 2005 June 13, *Geophys. J. Int.*, *167*, 838–844, doi:10.1111/j.1365-246X.2006.03190.x.

Le Pichon, A., K. Antier, Y. Cansi, B. Hernandez, E. Minaya, B. Burgoa, D. P. Drob, L. G. Evers, and J. Vaubaillon (2008), Evidence for a meteoritic origin of the September 15, 2007, Carancas crater, *Meteorit. Planet. Sci.*, *43*, 1797–1809, doi:10.1111/j.1945-5100.2008.tb00644.x.

Le Pichon, A., J. Vergoz, E. Blanc, J. Guilbert, L. Ceranna, L. G. Evers, and N. Brachet (2009), Assessing the performance of the International Monitoring System's infrasound network: Geographical coverage and temporal variabilities, *J. Geophys. Res.*, *114*, D08112, doi:10.1029/2008JD010907.

Longuet-Higgins, M. S. (1950), A theory of the origin of microseisms, *Philos. Trans. R. Soc. London, Ser. A*, *243*, 1–35, doi:10.1098/rsta.1950.0012.

Manney, G. L., et al. (2008), The evolution of the stratopause during the 2006 major warming: Satellite data and assimilated meteorological analyses, *J. Geophys. Res.*, *113*, D11115, doi:10.1029/2007JD009097.

Marchetti, E., M. Ripepe, A. J. L. Harris, and D. Delle Donne (2009), Tracing the differences between Vulcanian and Strombolian explosions using infrasonic and thermal radiation energy, *Earth Planet. Sci. Lett.*, *279*(3–4), 273–281, doi:10.1016/j.epsl.2009.01.004.

Matoza, R., M. A. H. Hedlin, and M. Garcés (2007), An infrasound array study of Mount St. Helens, *J. Volcanol. Geotherm. Res.*, *160*(3–4), 249–262, doi:10.1016/j.jvolgeores.2006.10.006.

Matoza, R., D. Fee, M. Garcés, J. M. Seiner, P. A. Ramon, and M. A. H. Hedlin (2009), Infrasonic jet noise from volcanic eruptions, *Geophys. Res. Lett.*, *36*, L08303, doi:10.1029/2008GL036486.

McKenna, M. H. B., B. Stump, S. Hayek, J. R. McKenna, and T. R. Stanton (2007), Tele-infrasonic studies of hard-rock mining explosions, *J. Acoust. Soc. Am.*, *122*, doi:10.1121/1.2741375.

McNutt, S. R. (2005), Volcanic seismology, *Annu. Rev. Earth Planet. Sci.*, *33*, 461–491, doi:10.1146/annurev.earth.33.092203.122459.

Migliorini, S., C. Piccolo, and C. D. Rodgers (2008), Use of the information content in satellite measurements for an efficient interface to data assimilation, *Mon. Weather Rev.*, *136*, 2633–2650, doi:10.1175/2007MWR2236.1.

Mikumo, R. (1968), Atmospheric pressure waves and tectonic deformation associated with the Alaskan earthquake of March 28, 1964, *J. Geophys. Res.*, *73*, 2009–2025, doi:10.1029/JB073i006p02009.

Modrak, R. T., S. J. Arrowsmith, and D. N. Anderson (2010), A Bayesian framework for infrasound location, *Geophys. J. Int.*, *181*, 399–405, doi:10.1111/j.1365-246X.2010.04499.x.

Moran, S. C. (1994), Seismicity at Mount St. Helens, 1987–1992: Evidence for repressurization of an active magmatic system, *J. Geophys. Res.*, *99*, 4341–4354, doi:10.1029/93JB02993.

Moran, S. C., P. J. McChesney, and A. B. Lockhart (2008), Seismicity and infrasound associated with explosions at Mount St. Helens, 2004–2006, in *A Volcano Rekindled: The Renewed Eruption of Mount St. Helens, 2004–2006*, edited by D. R. Sherrod, W. E. Scott, and P. H. Stauffer, *U.S. Geol. Surv. Prof. Pap.*, *1750*, 111–128.

Mori, J., H. Patia, C. McKee, I. Itikarai, P. Lowenstein, P. De Saint Ours, and B. Talai (1989), Seismicity associated with eruptive activity at Langila Volcano, Papua New Guinea, *J. Volcanol. Geotherm. Res.*, *38*, 243–255, doi:10.1016/0377-0273(89)90040-1.

Murayama, Y., K. Igarashi, D. D. Rice, B. J. Watkins, R. L. Collins, K. Mizutani, Y. Saito, and S. Kainuma (2000), Medium frequency radars in Japan and Alaska for upper atmosphere observations, *IEICE Trans. Commun.*, *E83-B*, 1996–2003.

Mutschlecner, J. P., and R. W. Whitaker (2005), Infrasound from earthquakes, *J. Geophys. Res.*, *110*, D01108, doi:10.1029/2004JD005067.

Mutschlecner, J. P., R. W. Whitaker, and L. H. Auer (1999), An empirical study of infrasound propagation, report, Los Alamos Natl. Lab., Los Alamos, N. M.

Negraru, P., P. Golden, and E. Herrin (2008), Dispersed infrasound signals in the "zone of silence," *Eos Trans. AGU*, *89*(53), Fall Meet. Suppl., Abstract S11B-1734.

Neuberg, J., R. Luckett, M. Ripepe, and T. Braun (1994), Highlights from a seismic broadband array on Stromboli volcano, *Geophys. Res. Lett.*, *21*(9), 749–752, doi:10.1029/94GL00377.

Oberheide, J., Q. Wu, T. L. Killeen, M. E. Hagan, and R. G. Roble (2006), Diurnal nonmigrating tides from TIMED Doppler Interferometer wind data: Monthly climatologies and seasonal variations, *J. Geophys. Res.*, *111*, A15S03, doi:10.1029/2005JA011491.

Olson, J. V. (2004), The application of the pure-state filter to infrasound array data, *InfraMatics*, *7*, 15–21.

Olson, J. V., C. R. Wilson, and R. A. Hansen (2003), Infrasound associated with the 2002 Denali fault earthquake, Alaska, *Geophys. Res. Lett.*, *30*(23), 2195, doi:10.1029/2003GL018568.

Oshima, H., and T. Maekawa (2001), Excitation process of infrasonic waves associated with Merapi-type pyroclastic flow as revealed by a new recording system, *Geophys. Res. Lett.*, *28*(6), 1099–1102, doi:10.1029/1999GL010954.

Pekeris, C. L. (1939), The propagation of a pulse in the atmosphere, *Proc. R. Soc. London A*, *171*, 434–449, doi:10.1098/rspa.1939.0076.

Picone, J. M., A. E. Hedin, D. P. Drob, and A. C. Aikin (2002), NRLMSISE-00 empirical model of the atmosphere: Statistical comparisons and scientific issues, *J. Geophys. Res.*, *107*(A12), 1468, doi:10.1029/2002JA009430.

Pierce, A. D., and W. A. Kinney (1976), Computational techniques for the study of infrasound propagation in the atmosphere, *Rep. AFGL-TR-76-56*, Air Force Geophys. Lab., Hanscom AFB, Mass.

Posmentier, E. S. (1967), A theory of microbaroms, *Geophys. J. R. Astron. Soc.*, *13*, 487–501.

Rabier, F. (2005), Overview of global data assimilation developments in numerical weather-prediction centres, *Q. J. R. Meteorol. Soc.*, *131*, 3215–3233, doi:10.1256/qj.05.129.

ReVelle, D. (1976), On meteor generated infrasound, *J. Geophys. Res.*, *81*, 1217–1229, doi:10.1029/JA081i007p01217.

Richter, J. H., F. Sassi, R. R. Garcia, K. Matthes, and C. A. Fischer (2008), Dynamics of the middle atmosphere as simulated by the Whole Atmosphere Community Climate Model, version 3 (WACCM3), *J. Geophys. Res.*, *113*, D08101, doi:10.1029/2007JD009269.

Rind, D. (1980), Microseisms at Palisades: 3. Microseisms and microbaroms, *J. Geophys. Res.*, *85*, 4854–4862, doi:10.1029/JB085iB09p04854.

Ripepe, M., and E. Marchetti (2002), Array tracking of infrasonic sources at Stromboli volcano, *Geophys. Res. Lett.*, *29*(22), 2076, doi:10.1029/2002GL015452.

Ripepe, M., A. J. L. Harris, and R. Carniel (2002), Thermal, seismic and infrasonic evidences of variable degassing rates at Stromboli volcano, *J. Volcanol. Geotherm. Res.*, *118*, 285–297, doi:10.1016/S0377-0273(02)00298-6.

Ripepe, M., S. De Angelis, G. Lacanna, P. Poggi, C. Williams, E. Marchetti, D. Delle Donne, and G. Ulivieri (2009), Tracking pyroclastic flows at Soufriere Hills Volcano, *Eos Trans. AGU*, *90*(27), 229–231, doi:10.1029/2009EO270001.

Ritsema, A. R. (1980), Observations of Mount St. Helens eruption, *Eos Trans. AGU*, *61*, 1201.

Rogers, R. M., A. Sauter, R. W. Busby, T. Kim, C. Hayward, and B. W. Stump (2008), Infrasound observations at USArray sites—A preliminary investigation of the utility of seismo-acoustic observations on a regional scale, *Eos Trans. AGU*, *89*(53), Fall Meet. Suppl., Abstract S33B-1944.

Romanowicz, B. (2003), Global mantle tomography: Progress status in the past 10 years, *Annu. Rev. Earth Planet. Sci.*, *31*, 303–328, doi:10.1146/annurev.earth.31.091602.113555.

Ruiz, M., J. M. Lees, and J. B. Johnson (2006), Source constraints of Tungurahua volcano explosion events, *Bull. Volcanol.*, *68*(5), 480–490, doi:10.1007/s00445-005-0023-8.

Schwartz, M. J., et al. (2008), Validation of the Aura Microwave Limb Sounder temperature and geopotential height measurements, *J. Geophys. Res.*, *113*, D15S11, doi:10.1029/2007JD008783.

She, C. Y. (2004), Initial full-diurnal-cycle mesopause region lidar observations: Diurnal-means and tidal perturbations of temperature and winds over Fort Collins, CO (41°N 105°W), *J. Atmos. Sol. Terr. Phys.*, *66*, 663–674, doi:10.1016/j.jastp.2004.01.037.

Shepherd, G. G., et al. (1993), WINDII, the Wind Imaging Interferometer on the Upper-Atmosphere Research Satellite, *J. Geophys. Res.*, *98*, 10,725–10,750, doi:10.1029/93JD00227.

Shields, F. D. (2005), Low-frequency wind noise correlation in microphone arrays, *J. Acoust. Soc. Am.*, *117*, 3489–3496, doi:10.1121/1.1879252.

Simmons, A., M. Hortal, G. Kelly, A. McNally, A. Untch, and S. Uppala (2005), ECMWF analyses and forecasts of stratospheric winter polar vortex breakup: September 2002 in the Southern Hemisphere and related events, *J. Atmos. Sci.*, *62*, 668–689, doi:10.1175/JAS-3322.1.

Strachey, R. (1888), On the air waves and sounds caused by the eruption of Krakatoa in August, 1883, in *The Eruption of Krakatoa and Subsequent Phenomena*, edited by G. J. Symons, pp. 57–88, Trubner, London.

Stump, B., M. A. H. Hedlin, D. C. Pearson, and V. Hsu (2002), Characterization of mining explosions at regional distances: Implications with the international monitoring system, *Rev. Geophys.*, *40*(4), 1011, doi:10.1029/1998RG000048.

Stump, B., M.-S. Jun, C. Hayward, J.-S. Jeon, I.-Y. Che, K. Thomason, S. M. House, and J. McKenna (2004), Small-aperture seismo-acoustic arrays: Design, implementation, and utilization, *Bull. Seismol. Soc. Am.*, *94*, 220–236, doi:10.1785/0120020243.

Stump, B., R. Burlacu, C. Hayward, J. Bonner, K. L. Pankow, A. Fisher, and S. Nava (2007), Seismic and infrasound energy generation and propagation at local and regional distances: Phase I: Divine Strake experiment, in *Proceedings of the 29th Monitoring Research Review: Ground-Based Nuclear Explosion Monitoring Technologies*, pp. 674-683, Natl. Nucl. Secur. Admin., Washington, D. C.

Stump, B., R.-M. Zhou, T. S. Kim, Y.-T. Chen, Z.-X. Yang, R. B. Herrmann, R. Burlacu, C. Hayward, and K. L. Pankow (2008), Shear velocity structure in NE China and characterization of infrasound wave propagation in the 1–210 kilometer range, in *Proceedings of the 2008 Monitoring Research Review: Ground-Based Nuclear Explosion Monitoring Technologies*, pp. 287-296, Natl. Nucl. Secur. Admin., Washington, D. C.

Sutherland, L. C., and H. Bass (2004), Atmospheric absorption in the atmosphere up to 160 km, *J. Acoust. Soc. Am.*, *115*, 1012-1032, doi:10.1121/1.1631937.

Taylor, S. R., S. J. Arrowsmith, and D. N. Anderson (2010), Detection of short time transients from spectrograms using scan statistics, *Bull. Seismol. Soc. Am.*, *100*(5A), 1940–1951, doi:10.1785/0120100017.

Toksöz, N. F., and A. Ben-Menahem (1964), Excitation of seismic surface waves by atmospheric nuclear explosions, *J. Geophys. Res.*, *69*, 1639–1648, doi:10.1029/JZ069i008p01639.

Vergniolle, S., G. Brandeis, and J.-C. Mareschal (1996), Strombolian explosions: 2. Eruption dynamics determined from acoustic measurements, *J. Geophys. Res.*, *101*(B9), 20,449–20,466, doi:10.1029/96JB01925.

Vergniolle, S., M. Boichu, and J. Caplan-Auerbach (2004), Acoustic measurements of the 1999 basaltic eruption of Shishaldin volcano, Alaska: Origin of Strombolian activity, *J. Volcanol. Geotherm. Res.*, *137*, 135–151.

Vincent, R. A., and D. Lesicar (1991), Dynamics of the equatorial mesosphere: First results with a new generation partial reflection radar, *Geophys. Res. Lett.*, *18*(5), 825–828, doi:10.1029/91GL00768.

Wexler, H., and W. A. Hass (1962), Global atmospheric pressure effects of the October 30, 1961, explosion, *J. Geophys. Res.*, *67*, 3875–3887, doi:10.1029/JZ067i010p03875.

Whipple, F. J. W. (1930), The great Siberian meteor and the waves, seismic and aerial, which it produced, *Q. J. R. Meteorol. Soc.*, *56*, 287–304.

Whitaker, R. W. (2007), Infrasound signals as basis for event discriminants, in *Proceedings of the 29th Monitoring Research Review: Ground-Based Nuclear Explosion Monitoring Technologies*, pp. 905–913, Natl. Nucl. Secur. Admin., Washington, D. C.

Whitaker, R. W. (2009), Infrasound signals from ground motion sources, in *Proceedings of the 2009 Monitoring Research Review: Ground-Based Nuclear Explosion Monitoring Technologies*, pp. 750–758, Natl. Nucl. Secur. Admin., Washington, D. C.

Whitaker, R. W., and D. E. Norris (2008), Infrasound propagation, in *Handbook of Signal Processing in Acoustics*, edited by D. Havelock, S. Kuwano, and M. Vorlander, pp. 1487–1496, Springer, New York, doi:10.1007/978-0-387-30441-0_82.

Whitaker, R. W., S. Noel, J. P. Mutschlecner, and M. Davidson (1992), Infrasonic monitoring of UGTs and earthquakes for discrimination, paper presented at DOE/LLNL Verification Symposium on Technologies for Monitoring Nuclear Tests Related to Weapons Proliferation, Los Alamos Natl. Lab., Las Vegas, Nev.

Willis, M., M. Garcés, C. Hetzer, and S. Businger (2004), Infrasonic observations of open ocean swells in the Pacific: Deciphering the song of the sea, *Geophys. Res. Lett.*, *31*, L19303, doi:10.1029/2004GL020684.

Wilson, C. R., J. V. Olson, C. A. L. Szuberla, S. R. Mc, T. G. Nutt, and D. P. Drob (2006), Infrasonic array observations at I53US of the 2006 Augustine volcano eruptions, *InfraMatics*, *13*, 11–25.

Woulff, G., and T. R. McGetchin (1976), Acoustic noise from volcanoes—Theory and experiment, *Geophys. J. R. Astron. Soc.*, *45*(3), 601–616.

Wu, W. S., R. J. Purser, and D. F. Parrish (2002), Three-dimensional variational analysis with spatially inhomogeneous covariances, *Mon. Weather Rev.*, *130*, 2905–2916, doi:10.1175/1520-0493(2002)130<2905:TDVAWS>2.0.CO;2.

Yamasato, H. (1997), Quantitative analysis of pyroclastic flows using infrasonic and seismic data at Unzen volcano, Japan, *J. Phys. Earth*, *45*(6), 397–416.

Yokoo, A., T. Tameguri, and M. Iguchi (2009), Swelling of a lava plug associated with a Vulcanian eruption at Sakurajima Volcano, Japan, as revealed by infrasound record: Case study of the eruption on January 2, 2007, *Bull. Volcanol.*, *71*(6), 619–630, doi:10.1007/s00445-008-0247-5.

Young, J. M., and G. E. Greene (1982), Anomalous infrasound generated by the Alaskan earthquake of 28 March 1964, *J. Acoust. Soc. Am.*, *71*, 334–339, doi:10.1121/1.387457.

Zumberge, M. A., J. Berger, M. A. H. Hedlin, R. Hilt, S. Nooner, and R. Widmer-Schnidrig (2003), An optical fiber infrasound sensor: A new lower limit on atmospheric pressure noise between 1 Hz and 10 Hz, *J. Acoust. Soc. Am.*, *113*, 2474–2479, doi:10.1121/1.1566978.

S. J. Arrowsmith, Los Alamos National Laboratory, PO Box 1663, Los Alamos, NM 87545, USA. (arrows@lanl.gov)

D. P. Drob, Space Science Division, U.S. Naval Research Laboratory, Code 7643, 4555 Overlook Ave. SW, Washington, DC 20375, USA.

M. A. H. Hedlin, Laboratory for Atmospheric Acoustics, Institute of Geophysics and Planetary Physics, Scripps Institution of Oceanography, University of California, San Diego, IGPP 0225, La Jolla, CA 92093-0225, USA.

J. B. Johnson, Department of Earth and Environmental Science, New Mexico Institute of Mining and Technology, 801 Leroy Pl., Socorro, NM 87801, USA.